



Evidence for the asynchronous retreat of large outlet glaciers in southeast Greenland at the end of the last glaciation



Laurence M. Dyke ^{a,*}, Anna L.C. Hughes ^b, Tavi Murray ^a, John F. Hiemstra ^a, Camilla S. Andresen ^c, Ángel Rodés ^d

^a Glaciology Group, Swansea University, Singleton Park, Swansea SA2 8PP, UK

^b Department of Earth Science, University of Bergen and Bjerknes Centre for Climate Research, Allégaten 41, N-5007 Bergen, Norway

^c Geological Survey of Denmark and Greenland, Department of Marine Geology and Glaciology, Øster Voldgade 10, DK-1350 Copenhagen K, Denmark

^d NERC-CIAC, Scottish Universities Environmental Research Centre, East Kilbride G75 0QF, UK

ARTICLE INFO

Article history:

Received 22 February 2014

Received in revised form

28 May 2014

Accepted 2 June 2014

Available online 22 July 2014

Keywords:

Greenland Ice Sheet

Southeast Greenland

¹⁰Be exposure dating

Fjord deglaciation

ABSTRACT

Recent rapid changes in the marine-terminating sectors of the Greenland Ice Sheet (GrIS) have prompted concerns about the future stability of the ice sheet. Long-term records of ice sheet behaviour provide valuable context to assess the magnitude of current change and may help resolve the mechanisms driving deglaciation. We report 23 new ¹⁰Be exposure ages which constrain the deglacial history of two large fjord systems in southeast (SE) Greenland. We compare our chronologies with existing data from the centre of the sector to examine the timing and style of deglaciation at a regional-scale. Glacial erratic ¹⁰Be exposure ages demonstrate that Kangerdlugssuaq Fjord deglaciated at ~11.8 ka at the end of the Younger Dryas (YD – 12.8–11.6 ka). Retreat at Kangerdlugssuaq Fjord coincided with known incursion of the warm Irminger Current (IC) onto the continental shelf; this is inferred to have initiated retreat. Comparison with recently published results from Sermilik Fjord and new ¹⁰Be ages from Bernstorffs Fjord indicates deglaciation occurred ~1 ka later in the south of the SE region. Sermilik Fjord (~10.9 ka) and Bernstorffs Fjord (~10.4 ka) deglaciated later; retreat likely occurred in response to dramatic climatic amelioration at the termination of the YD stadial. We suggest that the disparate timing of deglaciation across the SE region may be primarily explained by the varying influence of the warm IC; glaciers in southern SE Greenland were isolated from warm Atlantic waters during the YD by complex shelf bathymetry. In all fjord settings ice retreat was rapid and persistent, consistent with the absence of geomorphological evidence for stillstand or readvance events. Ice retreat was accompanied by rapid thinning and likely continued to well within present-day ice sheet margins. Glacial erratic ¹⁰Be age determinations and geomorphological observations show no evidence for Holocene readvance events prior to the Little Ice Age (LIA).

© 2014 The Authors. Published by Elsevier Ltd. This is an open access article under the CC BY license ([//creativecommons.org/licenses/by/3.0/](http://creativecommons.org/licenses/by/3.0/)).

1. Introduction

Recent glaciological changes in southeast (SE) Greenland (Fig. 1) highlight the importance of the sector to the overall mass balance of the Greenland Ice Sheet (GrIS). In the first decade of the 21st century marine-terminating outlet glaciers across the region accelerated, thinned and then retreated simultaneously, apparently in response to regional-scale forcing(s) (Krabill et al., 1999; Howat et al., 2008; Thomas et al., 2009; Murray et al., 2010; Moon et al.,

2012; Straneo and Heimbach, 2013). Dynamic thinning has been shown to penetrate far inland, resulting in enhanced regional mass loss which now dominates the mass balance of the wider GrIS (Rignot and Kanagaratnam, 2006; Pritchard et al., 2009; Sasgen et al., 2012). Assessing the magnitude of current glaciological changes requires a well-defined ‘baseline’ beyond the record of historical observations and measurements. Techniques such as cosmogenic isotope dating enable reconstruction of glacier behaviour over long timescales and are valuable for understanding the response of the GrIS to external forcings. Detailed regional chronologies may also allow the identification of the individual driving mechanism(s) of deglaciation (e.g. Roberts et al., 2010, 2013; Larsen et al., 2013). Furthermore, records of palaeo-ice sheet behaviour are important for testing numerical ice sheet

* Corresponding author.

E-mail addresses: l.dyke.330856@swansea.ac.uk, [\(L.M. Dyke\).](mailto:330856@swansea.ac.uk)

models which attempt to predict the future behaviour of the GrIS (Simpson et al., 2009; Vinther et al., 2009). Despite its current significance to the overall mass balance of the GrIS, relatively little is known about the glacial history of the SE coast and it remains one of the least investigated regions of Greenland. Recently published results from the centre of the sector demonstrate that the area around Sermilik Fjord deglaciated at ~10.9 ka and that retreat was both rapid and sustained (Jakobsen et al., 2008; Long et al., 2008; Roberts et al., 2008; Hughes et al., 2012).

The deglacial history of the rest of the region is largely unknown. Terrestrial areas are particularly poorly represented; this reflects the predominantly erosional landscape which offers few opportunities for ^{14}C dating. Understanding the behaviour of large, high-discharge outlet glaciers is important as their history is intrinsically linked to the fate of the wider GrIS. Simple questions remain unanswered; it is not known when glaciers across the region retreated, how rapidly they deglaciated or which driver(s) paced retreat. We present new ^{10}Be exposure ages from Kangerdlugssuaq Fjord and Bernstorffs Fjord, the drainage portals for two of the largest glaciers in SE Greenland (Fig. 1). This enables investigation of the timing and style of deglaciation across the sector.

2. Study area – Southeast Greenland

The SE region covers 1500 km of coastline from Kap Farvel in the south to Kap Brewster at the entrance to Scoresby Sund (Fig. 1). The region is heavily glaciated; large tidewater outlet glaciers drain ~173,000 km² of the GrIS through long fjord systems incised into the coastline (Rignot and Kanagaratnam, 2006). Numerous independent mountain glaciers exist in the narrow, alpine coastal belt and in many locations the ice sheet margin sits directly at the modern coastline (Dwyer, 1995; Kelly and Long, 2009). Unglaciated terrain is predominantly characterised by ice-scoured bedrock; vegetation is sparse and limited to favourable locations (Humlum and Christiansen, 2008). The continental shelf is 60–200 km wide and typically a few hundred metres deep (Murray et al., 2010). Terrestrial fjord systems continue onto the continental shelf as transverse troughs up to 900 m deep; these generally shallow towards the shelf-break (Andrews et al., 1996; Kuijpers et al., 2003).

The modern SE region spans sub-Arctic to Arctic climate zones. Stable high-pressure conditions prevail during spring and summer, while low-pressure cells track the SE coast delivering heavy precipitation during autumn and winter (Hastings, 1960; Ohmura and Reeh, 1991). The SE region records the highest accumulation of the GrIS (Bales et al., 2009); this is offset by an ablation rate of ~6 m a⁻¹ at sea-level between 60 and 68°N (Reeh et al., 1999). The climate of the SE region is regulated by the GrIS and by cold southerly flowing ocean currents (Fig. 1). The coastal currents of SE Greenland form the north-eastern limb of the Subpolar Gyre: a broad anticlockwise circulation feature which partly regulates heat and salinity delivery in the North Atlantic (Aagaard and Coachman, 1968a, b; Hátún et al., 2005; Thornalley et al., 2009). The East Greenland Current (EGC) and its inner-shelf extension, the East Greenland Coastal Current (EGCC), are cool, low-salinity, high-velocity surface currents (Sutherland and Pickart, 2008). These currents are augmented by glacial ice and meltwater from the GrIS (Bacon et al., 2002; Sutherland and Pickart, 2008). The Irminger Current (IC) flows at depth beneath a ‘cap’ of Arctic water and delivers warm, saline water from the subtropics (Straneo et al., 2010; Bearley et al., 2012; Sutherland et al., 2013). The IC penetrates the deepest troughs and fjords, reaching at least some outlet glacier termini (Murray et al., 2010; Straneo et al., 2010; Christoffersen et al., 2012).

2.1. Sampling sites – Kangerdlugssuaq Fjord and Bernstorffs Fjord

This study focusses on two large fjord systems in the SE region (Figs. 1 and 3). The fjords are situated 750 km apart; approximately equal distances north and south of Sermilik Fjord, the subject of similar investigation (Hughes et al., 2012).

Kangerdlugssuaq Fjord, in the north of the sector, is ~70 km long, up to 12 km wide and headed by the marine-terminating Kangerdlugssuaq Glacier. The glacier is the largest of the sector, draining ~30% of the SE GrIS and discharging ~28 km³ of ice annually (Rignot and Kanagaratnam, 2006). Kangerdlugssuaq is one of the fastest outlet glaciers of the GrIS; velocities near the calving front can exceed 30 m day⁻¹ (Luckman et al., 2006; Murray et al., 2010). The glacier drains through a deep bedrock trough which extends ~40 km inland below sea-level (Bamber et al., 2013). Several smaller outlet glaciers drain into the main fjord through tributary fjords and numerous cirque glaciers and glacierets occupy favourable locations on the fjord walls which rise to >2000 m above sea-level (asl) (Schjøtt, 2007a). The bathymetry of the fjord is characterised by a featureless, steep-walled basin which deepens to a maximum of 870 m near the mouth (Dowdeswell et al., 2010). The surface bedrock of Kangerdlugssuaq Fjord is very diverse and is underpinned by reworked Archaean gneiss of the Nagssugtoqidian mobile belt (Nutman et al., 2008 – Fig. 1). Palaeogene flood basalts lie to the north and east (Nielsen et al., 1981) and several significant gabbro intrusions border the fjord. Additionally, an intense swarm of coast-parallel mafic dykes dissect the area; these were emplaced during the opening of the North Atlantic (Wager and Deer, 1938; Myers, 1980). The landscape is predominantly erosional and is characterised by ice-scoured, striated bedrock. Minor ‘fresh’ moraines are associated with cirque and valley glaciers and are assumed to delineate Little Ice Age (LIA) extent, as elsewhere in the region (Fristrup, 1970; Hasholt, 2000; Kelly and Lowell, 2009).

Bernstorffs Fjord, in the south of the sector, is part of a complex of geometrically similar east-west trending fjords which drain ice from a large plateau beneath the southern dome of the GrIS (Bamber et al., 2013). Bernstorffs Glacier drains a smaller catchment than Kangerdlugssuaq Glacier, yet high accumulation rates (~80 g cm⁻² a⁻¹) sustain velocities of up to 13 m day⁻¹ near the calving front (Bales et al., 2009; Murray et al., 2010). The fjord is ~50 km long and up to 7 km wide; steep mountains rise to >1500 m asl forming the fjord walls (Schjøtt, 2007b). A complex of three glaciers discharge into the head of the fjord. These directly drain the GrIS and are thought to have coalesced during the last glaciation to form an ice stream in the fjord. Detailed bathymetry is not available for the fjord; limited echo-sounding data show areas >800 m below sea-level (bsl) in the main fjord and no significant shoaling to at least Ensomheden Island (Fig. 3; unpublished GLIMPSE cruise data, 2011). The bathymetric data also show a prominent sill (~250 m bsl) at the mouth of Bernstorffs Fjord. Numerous grounded icebergs prevented bathymetric surveying here but we consider it likely that the sill runs the full width of the fjord mouth (unpublished GLIMPSE cruise data, 2011). Ensomheden Island lies in the middle of the fjord 35 km from the mouth and is ~250 m asl at its highest point (Schjøtt, 2007b). A well-defined line of grounded icebergs (observed in 2011) and a partly visible submerged moraine indicate that the northern passage around Ensomheden Island is very shallow (Fig. 2C). High-resolution aerial photos reveal this is the extension of a ‘fresh’ cirque glacier moraine, exhibiting a well-defined ridge line and a lack of vegetation (A. Bjørk, personal communication). Cirque and valley glaciers through the fjord are associated with similar moraines. These are assumed to have formed during the LIA. Bernstorffs Fjord lies

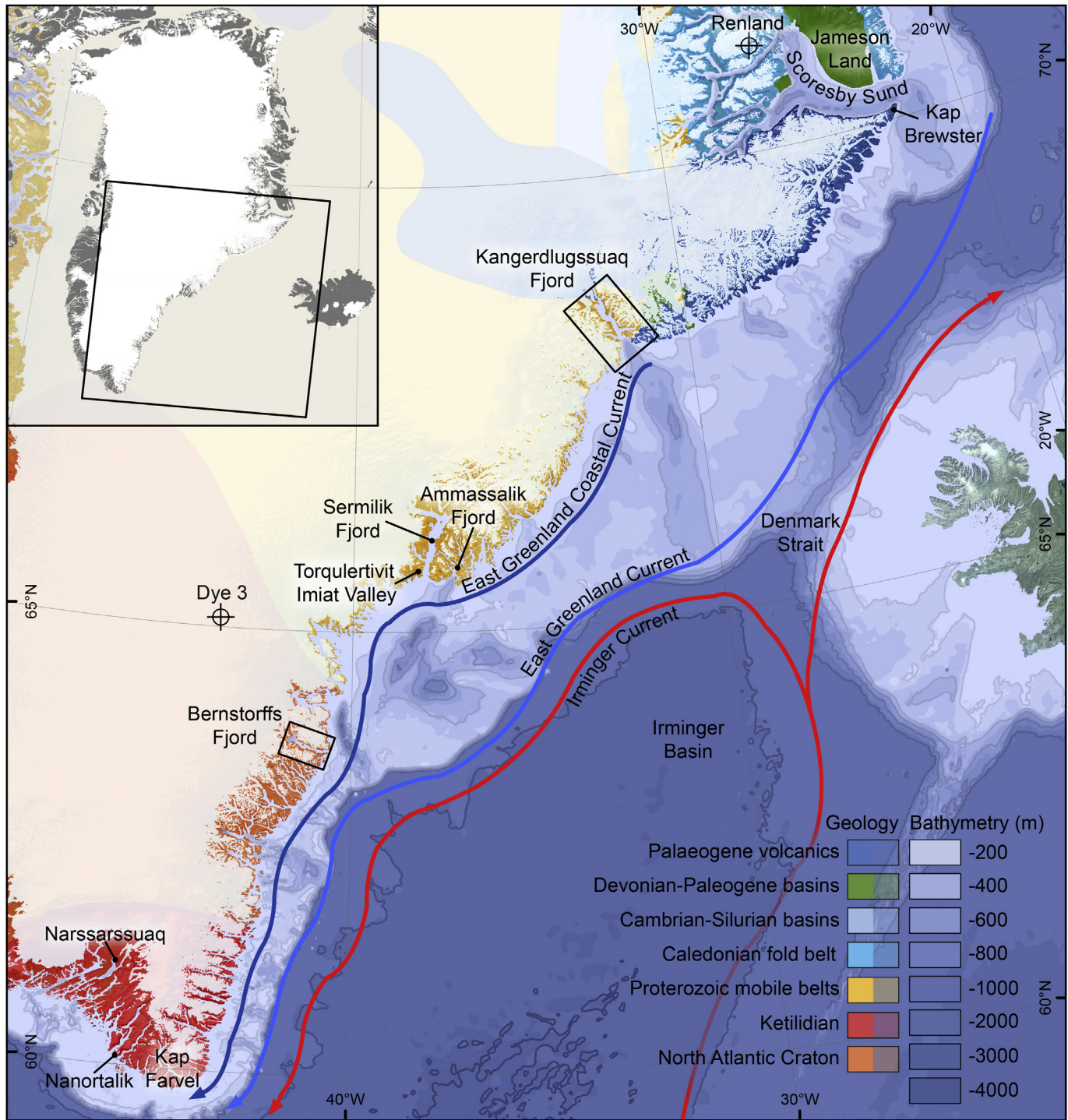


Fig. 1. Southeast Greenland 1:8,000,000. Inset map shows extent of main figure. Bathymetric data are from IBCAO v3.0 (Jakobsson et al., 2012) and GEBCO (IOC, IHO and BODC, 2003). Major regional ocean currents adapted from Sutherland and Pickart (2008). Terrestrial imagery is a composite mosaic of Landsat ETM + scenes downsampled to 250 m resolution (<http://zulu.ssc.nasa.gov/mrsid/>). Geological provinces and inferred sub-ice geology from Dawes (2009). Ice cores shown by crosses, boxes indicate extent of maps in Fig. 3.

within the North Atlantic Craton; the surface bedrock is primarily composed of Archaean gneisses, although large basaltic dykes of Proterozoic age invade country rock in some locations (Henriksen et al., 2000; Dawes, 2009). The fjord is characterised by scoured, streamlined bedrock and sparse vegetation cover. Small stands of willow (*Salix*) and birch (*Betula*) are indicative of milder climatic conditions than further north.

2.2. The late Quaternary in SE Greenland

The palaeoglaciology of the SE sector remains sparsely investigated; existing studies from across the region are summarised below. Published ^{10}Be exposure ages are recalculated using the Arctic production rate (Young et al., 2013) and Lal/Stone time-independent scaling (Lal, 1991; Stone, 2000). Radiocarbon ages

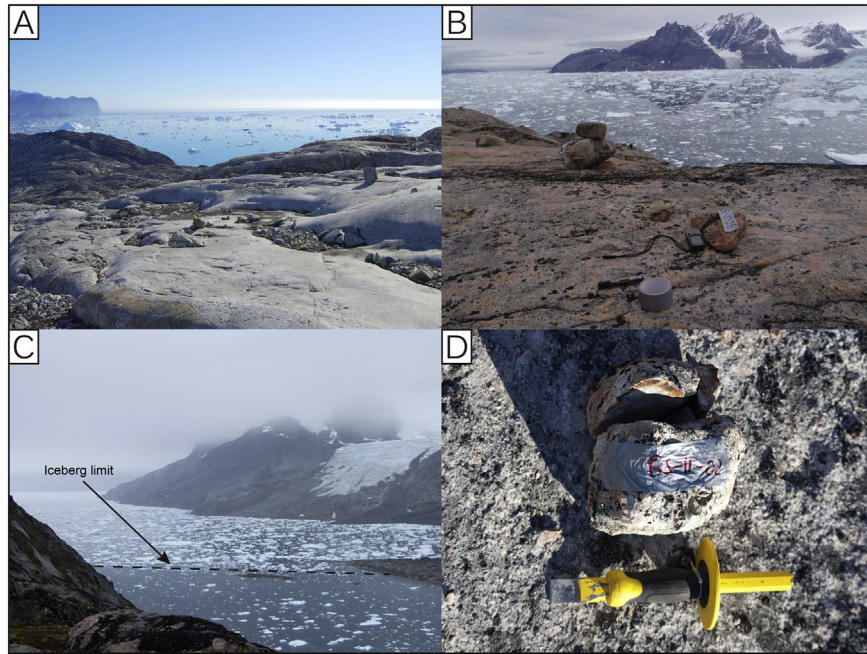


Fig. 2. Sampling site photos. A – Glacially polished, striated bedrock at KF1011 sampling site, view east across the mouth of Kangerdlugssuaq Fjord. B – Sample KF1025 near the head of Kangerdlugssuaq Fjord (view south). C – Ensomheden Island, Bernstorffs Fjord, sampling location for BS1110, BS1111 and BS1112 (view west). Note partially submerged moraine in fjord and clear iceberg limit. D – Typical erratic cobble sample (BS1102) from Bernstorffs Fjord, chisel for scale (31 cm long).

are recalibrated using CALIB 7.0 (Stuiver et al., 2005) and INTCAL13 or MARINE13 (Reimer et al., 2013) for terrestrial and marine radiocarbon ages respectively. A reservoir correction of 400 years is applied to marine radiocarbon dates (Jennings et al., 2006, 2011). Radiocarbon ages are shown as the median of 2σ calibrated age range with 2σ error.

2.2.1. The Last Glacial maximum

Sandurs and ‘fresh’ moraine ridges identified from early bathymetric charts (Iverson, 1936) suggest the GrIS extended to the shelf-edge during the Last Glacial (Sommerhoff, 1981). This interpretation is supported by subsequent research which documented ‘stiff’ over-consolidated tills (Mienert et al., 1992; Larsen et al., 1994; Lykke-Andersen, 1998; Jennings et al., 2006), constructional ‘moraine’ features (Svitski et al., 1999) and subglacial landforms (Dowdeswell et al., 2010) on outer-shelf areas.

Very little is known about the vertical extent of the GrIS during the Last Glacial. Glacially eroded surfaces and erratics exist to at least 1200 m asl in Kangerdlugssuaq Fjord; demonstrating a period of thick ice cover (Brooks, 1979), however, these lack dating constraint. Bedrock ^{10}Be and ^{26}Al exposure ages from the mouth of Sermilik Fjord reveal that ice reached up to at least 740 m asl there, and was likely much thicker (Roberts et al., 2008).

At maximum extent approximately 200,000 km² of ice had built up on the continental shelf of SE Greenland (Funder et al., 2011). Shelf ice is thought to have been highly dynamic with persistent ice streams forming in the major troughs and areas of convergent ice flow (Dowdeswell et al., 2010; Funder et al., 2011).

2.2.2. Deglaciation

Existing deglacial chronologies from across the SE region are briefly summarised below; working systematically south from Scoresby Sund to Kap Farvel (Fig. 1).

A pronounced increase in $\delta^{18}\text{O}$ values, changes in sedimentation and a reduction in sea ice are collectively interpreted as marking the onset of deglaciation off Scoresby Sund at ~15.8 cal ka BP (Nam et al., 1995; Stein et al., 1996). ^{10}Be exposure ages suggest earlier

deglaciation at Kap Brewster (~16.6 ka) and further north in Jameson Land (~18.5 ka), although nuclide inheritance may complicate this interpretation (Håkansson et al., 2007, 2011). Lacustrine ^{14}C dates and ^{10}Be exposure ages suggest the main body of Scoresby Sund deglaciated at around 11 ka (Funder, 1978; Björck et al., 1994; Cremer et al., 2001; Hall et al., 2008a; Levy et al., 2013; Lowell et al., 2013).

Sediment core data indicate deglaciation of the outer-continental shelf off Kangerdlugssuaq Fjord at ~17 cal ka BP (Andrews et al., 1997; Jennings et al., 2006). Radiocarbon dates from the length of Kangerdlugssuaq Trough provide minimum constraints on deglaciation and indicate ice retreat from the outer-shelf by 17–14 cal ka BP and the inner-shelf by ~13–11 cal ka BP (Mienert et al., 1992; Andrews et al., 1997; Jennings et al., 2002a, 2006). High-resolution bathymetry and TOPAS data show no evidence for stillstand or readvance events; suggesting that deglaciation was continuous to the inner-shelf (Dowdeswell et al., 2010). A depositional feature on the sill separating Kangerdlugssuaq Trough from the inner-shelf basin and fjord is interpreted as a moraine (Fig. 5) which formed as the ice margin stabilised on the bathymetric high (Stein, 1996; Andrews et al., 1997). Final retreat from the continental shelf occurred sometime between 13.6 and 11.5 cal ka BP (Smith et al., 2001; Jennings et al., 2002a, 2006).

Recently reported radiocarbon and cosmogenic isotope exposure ages from around Sermilik Fjord (Fig. 1) form the only terrestrial deglacial chronology for the 1500 km of coastline from Scoresby Sund to Kap Farvel (Jakobsen et al., 2008; Long et al., 2008; Roberts et al., 2008; Hughes et al., 2012). Recalculated bedrock ^{10}Be exposure ages from Torqulertivit Imit Valley, at the mouth of Sermilik Fjord, indicate ice retreat at ~12.4 ka (Roberts et al., 2008). ^{10}Be exposure ages from erratics spanning the full length of Sermilik Fjord illustrate that rapid ($\sim 80 \text{ m a}^{-1}$), continuous retreat occurred at ~10.9 ka (Hughes et al., 2012). Radiocarbon dates from the neighbouring Ammassalik Fjord demonstrate the onset of lacustrine organic sedimentation at ~11 cal ka BP (Long et al., 2008); suggesting synchronous deglaciation of fjord systems in this locality (Fig. 1).

Continental shelf deglaciation in the south of the sector appears to have occurred broadly synchronously with areas further north.

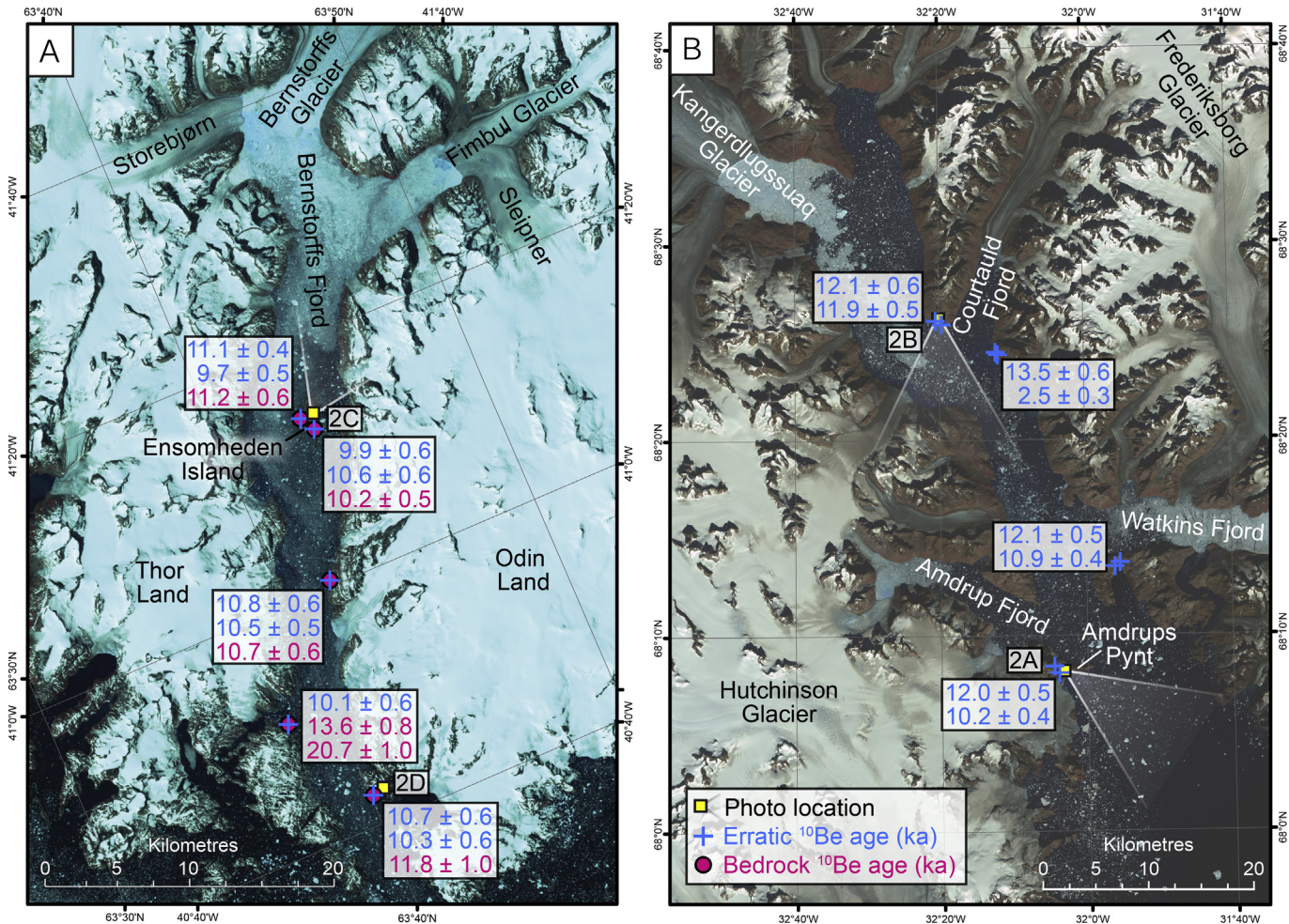


Fig. 3. Fjord ^{10}Be chronology. A – Bernstorffs Fjord. B – Kangerdlugssuaq Fjord. ^{10}Be exposure ages are reported in thousands of years (ka) with internal uncertainties. Camera position and field of view (where relevant) for photographs in Fig. 2 are shown. Background imagery – pan-sharpened, false-colour Landsat ETM + scenes (<http://glovis.usgs.gov/>).

A core from the continental slope off Bernstorffs Fjord shows a pronounced increase in $\delta^{18}\text{O}$ values just prior to 16.0 cal ka BP, which likely reflects a large input of GrIS meltwater (Kuijpers et al., 2003). A reduction in sedimentation on the mid-shelf reflects ice margin recession and the initiation of glaciomarine conditions here by ~14.7 cal ka BP (Kuijpers et al., 2003).

Deglaciation in southernmost Greenland may have initiated as early as 19 cal ka BP (Carlson et al., 2008). Increased $\delta^{18}\text{O}$ values off Kap Farvel suggest deglaciation was well established by 16.9 cal ka BP (Stoner et al., 1995), although this may reflect the southerly advection of meltwater from the SE region. The ice margin reached the outer coast at Nanortalik (Fig. 1) at ~14 cal ka BP (Bennike, 2002). Relative sea-level curves indicate gradual retreat from 14 to 12 cal ka BP, and a period of accelerated glacier retreat between 12 and 9 cal ka BP (Sparrenbom et al., 2006). Glaciers withdrew within current margins by 10.8 cal ka BP (Larsen et al., 2011).

3. Sampling design and preparation

3.1. Sampling design

Paired bedrock and erratic samples were collected from low-elevation lateral transects in Kangerdlugssuaq and Bernstorffs Fjords (Fig. 3). Transects extended from the outer-coast to the closest navigable position to the present-day ice margin. Both fjords contain numerous tributary glaciers; consequently sampling

locations were carefully chosen to reflect deglaciation of the main trunk of each fjord. Collecting samples from low-elevation fjord axis transects permits reconstruction of both the onset of deglaciation and the rate of subsequent glacier retreat. Both bedrock and erratic samples from Bernstorffs Fjord were analysed to investigate nuclide inheritance and potential multiple event histories (Briner et al., 2009; Corbett et al., 2011; Hughes et al., 2012).

3.2. Sampling methods

Paired erratic and bedrock samples were collected or removed using a hammer and chisel. All sites were located above the local marine limit, identified by the lowest occurrence of perched erratics (e.g. Long et al., 2008). Bedrock samples were taken from flat, ice-scoured surfaces (e.g. Fig. 2A). In most cases the topmost 5–10 cm were collected; thicker samples were cut to <10 cm prior to processing. Erratic samples typically consist of well-rounded cobbles (e.g. Fig. 2D). All samples were collected from quartz-rich gneisses (Table 1). Sample sites were generally located away from overshadowing steep slopes to avoid sampling remobilised clasts or postglacial slope deposits. Samples were collected from prominent bedrock flanks and ridges at low elevations. These areas would have been subject to maximum subglacial erosion, and thus isotopic inheritance from previous periods of exposure is minimised. Furthermore, snow accumulation is intrinsically limited on exposed ridges which mitigates snow shielding uncertainties. Position and

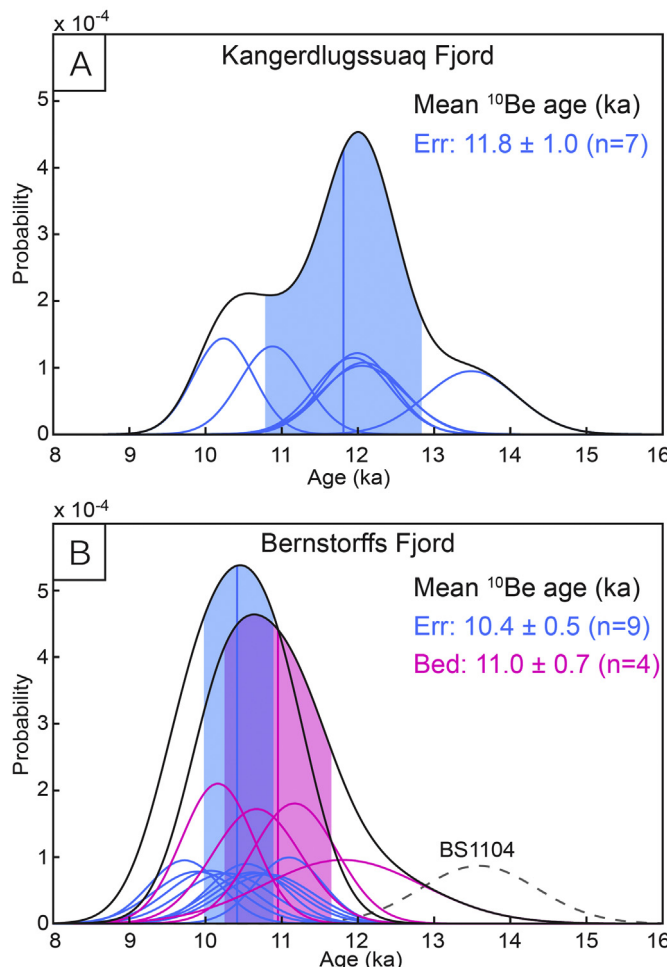


Fig. 4. Relative probability ('camel') plots after Balco (2011). A – Kangerdlugssuaq Fjord, B – Bernstorffs Fjord. Erratics shown in blue, bedrock samples in magenta. Coloured lines show individual exposure ages with internal uncertainties. Thick line denotes sum of all samples (excluding KF1021, BS1104 and BS1106 – see text for details). Vertical lines and shading show fjord means with 1σ area. (For interpretation of the references to colour in this figure legend, the reader is referred to the web version of this article.)

elevation were determined using a hand-held GPS unit with a horizontal uncertainty of ~5 m and elevation uncertainty of ~10 m. Topographic shielding was determined at 30° intervals using a compass and Suunto sighting clinometer.

3.3. Sample preparation and ^{10}Be measurement

Physical processing and acid etching were undertaken following methods outlined in Kohl and Nishizumi (1992). Quartz purity was checked by inductively coupled plasma optical emission spectrometry (ICP-OES) Al, Ca, Fe, and Ti determinations at the Scottish Universities Environmental Research Centre (SUERC, East Kilbride, UK). Between 15 and 25 g of clean quartz per sample were then dissolved in HF and spiked with ~200 mg of ^9Be carrier. The carrier used at the CIAF yields an average concentration of $2.7 \cdot 10^{-15} \pm 0.9 \cdot 10^{-15}$ $^{10}\text{Be}/^9\text{Be}$. BeO targets were prepared for $^{10}\text{Be}/^9\text{Be}$ analysis using ion exchange chromatography and following procedures modified from Child et al. (2000) at the Cosmogenic Isotope Analysis Facility (CIAF, SUERC, UK). $^{10}\text{Be}/^9\text{Be}$ ratios were measured with the 5 MV Pelletron AMS at the SUERC (Xu et al., 2010). Ratios were normalized to NIST SRM 4325 with a $^{10}\text{Be}/^9\text{Be}$ ratio of $2.79 \cdot 10^{-11}$, in agreement with those prepared by Nishizumi et al. (2007), which were used as secondary standards. Secondary standard

measurements scattered less than 3%. The sample $^{10}\text{Be}/^9\text{Be}$ ratios ranged between $5.8 \cdot 10^{-14}$ and $1.4 \cdot 10^{-13}$. Processed blank ratios ranged from 3 to $5 \cdot 10^{-15}$ and were subtracted from the measured ratios. The blank run alongside samples from Bernstorffs Fjord returned an unusually high ($1.7 \cdot 10^{-14}$) $^{10}\text{Be}/^9\text{Be}$ measurement. Samples from Bernstorffs Fjord were corrected using the mean blank ratio from all ^{10}Be blanks measured at the CIAF during 2012 ($4.3 \pm 1.3 \cdot 10^{-15}$ $^{10}\text{Be}/^9\text{Be}$) rather than the anomalous blank. ^{10}Be age determinations corrected using the CIAF blank mean are ~1.5 ka older and are more tightly grouped than those based on the anomalous blank measurement. This is consistent with a single abnormal blank reading rather than a systematic ^{10}Be contamination. Samples from Kangerdlugssuaq Fjord were corrected using the accompanying blank ($4.3 \pm 1.3 \cdot 10^{-15}$ $^{10}\text{Be}/^9\text{Be}$).

3.4. Exposure age calculation

Exposure ages were calculated with the CRONUS-earth online calculator (<http://hess.ess.washington.edu/math/> – version 2.2), using the Arctic production rate (Young et al., 2013) and time-independent Lal/Stone scaling scheme (Lal, 1991; Stone, 2000). Corrections were applied for sample thickness, density and topographic shielding (Table 1). Samples were not corrected for snow shielding as sampling sites were located in areas where snow accumulation is minimal (see 3.2). No correction for postglacial isostatic rebound was applied. Relative sea-level curves from the region indicate uplift occurred rapidly in the early Holocene (Long et al., 2008); consequently elevation corrections would be minor. Samples from across the region are also likely to have been subject to similar isostatic histories; this permits regional comparisons without uplift corrections. Elevation corrections for sites in West Greenland (Young et al., 2011b) are comparable to hand-held GPS vertical uncertainties (± 10 m). Applying an elevation correction of ~10 m to our data returns ages ~1.1% older, i.e. well within AMS measurement uncertainty. Samples were collected from glacially scoured crystalline gneiss (Fig. 2A). Micro-scale striations and glacially polished surfaces are preserved, indicating that bedrock is extremely resistant to erosion. Exposure ages are presented without applying an erosion correction. Calculating exposure ages using erosion rates of 1 mm ka^{-1} and 2 mm ka^{-1} yields ages ~1% and ~2% older respectively.

Exposure ages are presented in thousands of years (ka) before sample collection (2010 for Kangerdlugssuaq Fjord and 2011 for Bernstorffs Fjord). Stated uncertainties relate to AMS measurement (internal); these can be used to investigate the relationship between samples from a single data set (e.g. Corbett et al., 2011). ^{10}Be exposure ages from Sermilik Fjord (Hughes et al., 2012) were prepared and analysed using the same procedures as our new exposure ages and are also shown with internal uncertainties. When making comparisons with samples from different regions or with independent proxy records, external uncertainties should be applied; these account for additional production rate and scaling scheme uncertainties (c. 2–3.7% for the Arctic rate – Young et al., 2013).

4. Results

We present 23 new ^{10}Be age determinations from Kangerdlugssuaq Fjord ($n = 8$) and Bernstorffs Fjord ($n = 15$) (Table 1, Fig. 3). Exposure ages were calculated using the Arctic production rate (Young et al., 2013) which yields results <0.08% younger than the north-eastern North America (NENA) rate (Balco et al., 2009) but with reduced external uncertainties. Full sample details and results of ^{10}Be analysis are displayed in Table 1. Using alternative scaling schemes alters absolute ages by <0.1–2.6% but, importantly, does not change the overall relative chronology (Table 2).

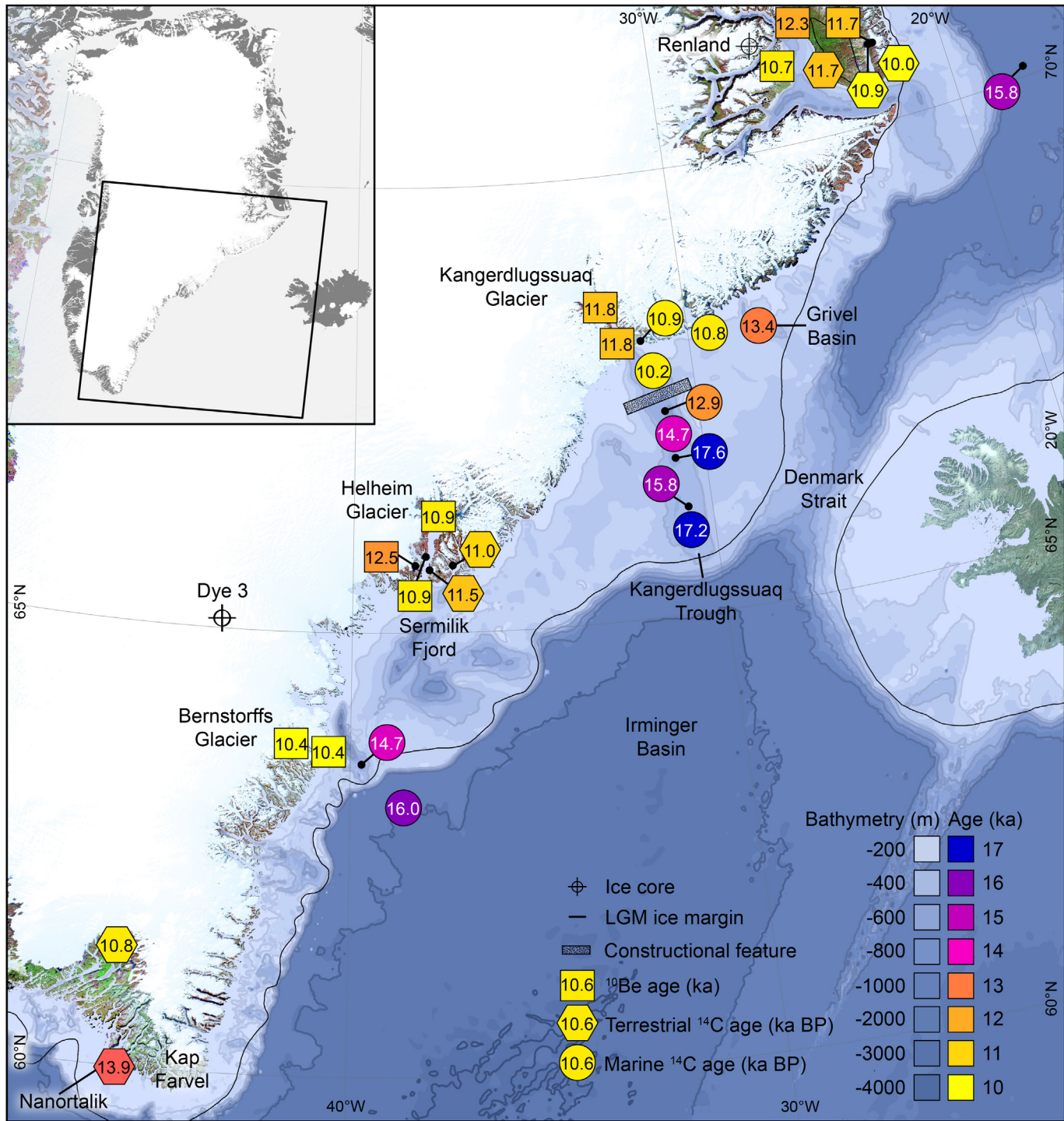


Fig. 5. Regional deglaciation chronology, for details see Table 3. Constructional feature from Andrews et al. (1997). Black line shows Last Glacial Maximum (LGM) ice limit from Funder et al. (2011). Inset map and box show location of figure. Multi-hue colour scales calculated using Bézier interpolation and lightness correction (e.g. Harrower and Brewer, 2003). (For interpretation of the references to colour in this figure legend, the reader is referred to the web version of this article.)

Individual ages are presented with internal uncertainties; mean sample ages are shown with uncertainties of ± 1 standard deviation.

4.1. Kangerdlugssuaq Fjord

Erratic samples ($n = 8$) were collected from low-elevation sites spanning 40 km of Kangerdlugssuaq Fjord (Fig. 3B). Exposure ages range from 10.2 ± 0.4 ka to 13.5 ± 0.6 ka (Table 1). Sample KF1021 (2.5 ± 0.3 ka) is considerably younger than the rest of the

population and is identified as an outlier using Peirce's criterion (Peirce, 1852; Ross, 2003). KF1021 met the sampling criteria as a perched and well-rounded clast (indicative of subglacial emplacement). However, the young ^{10}Be age suggests a more complex history. We exclude KF1021 from further analysis.

Samples do not exhibit any pattern in terms of distance from the fjord mouth and there is age variation even within individual sampling sites (see Figs. 3 and 4 and Table 1). The youngest (10.2 ± 0.4 ka) age occurs at the mouth of the fjord, the oldest

Table 1

Sample details and ^{10}Be age determinations, exposure ages are calculated using the Arctic production rate (Young et al., 2013) and Lal/Stone time-independent scaling (Lal, 1991; Stone, 2000).

Sample name	AMS ID	Lat. ($^{\circ}\text{N}$) ^a	Long. ($^{\circ}\text{W}$)	Elevation (m asl)	Sample type	Lithology	Thickness (cm)	Density (g cm^{-3}) ^b	Shielding correction ^c	^{10}Be (atoms/g)	^{10}Be uncert. (atoms/g)	Exposure age (yr)	Int. error (yr)	Ext. error (yr)
Kangerdlugssuaq Fjord														
KF1003	b5043	68.138	-32.066	178	Erratic	Gneiss	5	2.73	0.9908	57,764	2249	11,993	468	656
KF1011	b5044	68.143	-32.059	209	Erratic	Gneiss	4.5	2.74	0.9695	50,077	1934	10,236	396	557
KF1016	b5045	68.222	-31.940	100	Erratic	Gneiss	8.1	2.81	0.9779	51,388	2248	12,076	530	703
KF1017	b5142	68.222	-31.940	87	Erratic	Gneiss	4.2	2.68	0.9797	47,321	1874	10,880	432	600
KF1021	b5143	68.409	-32.210	78	Erratic	Gneiss	5.9	2.88	0.9274	10,178	1278	2542	319	334
KF1022	b5145	68.409	-32.210	75	Erratic	Banded gneiss	7.2	2.67	0.9274	53,308	2369	13,485	601	792
KF1024	b5146	68.432	-32.335	116	Erratic	Banded gneiss	5.5	2.69	0.9915	53,777	2462	12,056	554	721
KF1025	b5147	68.432	-32.334	115	Erratic	Pink gneiss	6.5	2.69	0.9915	52,760	2187	11,935	496	674
Bernstorffs Fjord														
BS1101	b5540	63.668	-40.711	113	Bedrock	Banded gneiss	4.4	2.68	0.9997	56,049	4941	11,803	1044	1137
BS1102	b5541	63.668	-40.711	111	Erratic	Pink gneiss	8.7	2.61	0.9997	49,154	2673	10,710	584	713
BS1103	b5542	63.668	-40.711	113	Erratic	Pink gneiss	9.6	2.68	0.9993	46,812	2666	10,272	587	706
BS1104	b5543	63.636	-40.849	75	Bedrock	Banded gneiss	7.1	2.68	0.9941	60,246	3391	13,587	767	927
BS1105	b5544	63.636	-40.850	73	Erratic	Gneiss	4.2	2.71	0.9949	45,618	2525	10,063	558	678
BS1106	b5546	63.637	-40.849	79	Bedrock	Banded gneiss	5.8	2.66	0.9949	93,197	4272	20,730	955	1243
BS1107	b5547	63.725	-41.214	237	Erratic	Gneiss	5.5	2.64	0.9989	57,449	3175	10,817	599	728
BS1108	b5572	63.725	-41.214	237	Erratic	Gneiss	5.7	2.68	0.9989	55,837	2616	10,537	495	638
BS1109	b5573	63.725	-41.214	237	Bedrock	Banded gneiss	5.5	2.72	0.9989	56,594	3070	10,670	580	709
BS1110	b5548	63.720	-41.231	89	Erratic	Gneiss	5.9	2.72	0.9976	44,845	2571	9889	568	683
BS1111	b5549	63.720	-41.231	89	Erratic	Gneiss	5.4	2.66	0.9976	48,366	2617	10,615	576	705
BS1112	b5576	63.720	-41.231	89	Bedrock	Banded gneiss	4.8	2.68	0.9976	46,516	2169	10,162	475	614
BS1113	b5552	63.695	-41.004	115	Erratic	Gneiss	6.85	2.69	0.9895	51,087	2049	11,096	446	616
BS1114	b5553	63.695	-41.004	115	Bedrock	Banded gneiss	6.2	2.67	0.9903	51,749	2559	11,169	554	699
BS1115	b5554	63.696	-41.004	115	Erratic	Gneiss	6.8	2.72	0.9896	44,777	2144	9724	467	597

^a Position and elevation from hand-held GPS units (uncertainty ± 10 m).

^b Density calculated from subsamples, fjord mean density used for KF1011, BS1101, BS1104 and BS1112.

^c Topographic shielding recorded *in situ* using compass and clinometer, shielding calculated online: http://hess.ess.washington.edu/math/general/skyline_input.php.

(13.5 ± 0.6 ka) is from the site close to the present-day ice margin. The site at the head of the fjord is the only location where ages are concordant within 1σ internal uncertainties (KF1024 – 12.1 ± 0.6 ka and KF1025 – 11.9 ± 0.5 ka). The cause of exposure age variation from within individual sampling sites remains unknown. Younger ages may result from localised shielding by perennial snow-patches or stagnant ice following deglaciation. The oldest sample (KF1022) may reflect a small degree of nuclide inheritance. Site-specific differences in snow or ice shielding are particularly likely on Amdrups Pynt at the mouth of the fjord. Samples here (KF1003 – 12.0 ± 0.5 ka and KF1011 – 10.2 ± 0.4 ka) were collected several hundred metres apart owing to a dearth of suitable erratic cobbles (Fig. 3). We suggest that the very tightly grouped central ^{10}Be ages (KF1024, KF1025, KF1003, KF1016 – mean 12.0 ± 0.1 ka) probably most accurately represent deglaciation; however, we use the similar fjord mean ($\sim 11.8 \pm 1.0$ ka) from the remaining 7 samples, as we cannot reasonably exclude the other ages. We calculate a very conservative average retreat rate of $\sim 10 \text{ m a}^{-1}$ using transect length (40 km) and 2σ range of sample average (after Briner et al., 2009), although retreat may have occurred over timescales as short as several hundred years.

4.2. Bernstorffs Fjord

Erratic ($n = 9$) and bedrock ($n = 6$) ^{10}Be exposure ages from Bernstorffs Fjord span 30 km and range from 9.7 ± 0.5 to

13.6 ± 0.8 ka (Fig. 3A). Sample BS1106 (20.7 ± 1.0) is identified as an outlier using Peirce's criterion (Peirce, 1852; Ross, 2003). This bedrock sample is interpreted as containing ^{10}Be from a previous period of exposure (e.g. Briner et al., 2008; Håkansson et al., 2009) and is excluded from further analysis. A paired bedrock sample (BS1104 – 13.6 ± 0.8 ka) from the same location is also excluded on the basis that erosion was insufficient to remove pre-existing isotope content at this location. An erratic sample (BS1105) from the site has an age of 10.1 ± 0.6 ka, concordant with erratic samples from the rest of the fjord, and is considered to accurately represent deglaciation. The mean of erratic samples from Bernstorffs Fjord is 10.4 ± 0.5 ka, the remaining bedrock samples return a mean of 11.0 ± 0.7 ka (Fig. 4). Bedrock and erratic populations cannot be differentiated using a *t*-test (two-tailed, unequal sample variance) which returns a *P* value of 0.232. Whilst the remaining bedrock ages probably provide a reasonable constraint on deglaciation, we suspect minor inheritance of ^{10}Be . Glacial erosion was apparently insufficient in some locations to completely remove pre-existing nuclide content, indicating erosion of less than ~ 2 m (Gosse and Phillips, 2001) through Marine Isotope Stage (MIS) 2. Consequently we calculate the timing and rate of deglaciation using erratic samples only. ^{10}Be exposure ages from erratics exhibit no spatial trend along the fjord and all overlap within 2σ . A conservative average retreat rate of 16 m a^{-1} is calculated using transect length (30 km) and 2σ range (after Briner et al., 2009). This is considered a minimum estimate.

Table 2

Exposure ages calculated using alternative spallation scaling schemes and Arctic production rate (Young et al., 2013). All other parameters remain the same as Table 1.

Scaling scheme		Desilets and Zreda (2003)/ Desilets et al. (2006)		Dunai (2001)		Lifton et al. (2005)		Lal (1991)/Stone (2000) time-dependent		Lal (1991)/Stone (2000) time-independent	
Sample ID	Type	Exposure age (ka)	External uncert. (a)	Exposure age (ka)	External uncert. (ka)	Exposure age (ka)	External uncert. (ka)	Exposure age (ka)	External uncert. (ka)	Exposure age (ka)	External uncert. (ka)
Kangerdlugssuaq Fjord											
KF1003	Erratic	11.9	0.7	11.9	0.7	12.0	0.7	12.0	0.7	12.0	0.7
KF1011	Erratic	10.2	0.6	10.2	0.6	10.2	0.6	10.2	0.6	10.2	0.6
KF1016	Erratic	11.9	0.7	11.9	0.7	12.0	0.7	12.1	0.7	12.1	0.8
KF1017	Erratic	10.7	0.6	10.7	0.6	10.8	0.6	10.9	0.6	10.9	0.7
KF1021	Erratic	2.5	0.3	2.5	0.3	2.5	0.3	2.5	0.3	2.5	0.3
KF1022	Erratic	13.3	0.8	13.3	0.8	13.3	0.8	13.5	0.8	13.5	0.9
KF1024	Erratic	11.9	0.7	11.9	0.8	12.0	0.8	12.1	0.7	12.1	0.8
KF1025	Erratic	11.8	0.7	11.8	0.7	11.9	0.7	11.9	0.7	11.9	0.8
Erratic Mean^a		11.7	0.7	11.7	0.7	11.7	0.7	11.8	0.7	11.8	0.8
Bernstorffs Fjord											
BS1101	Bedrock	11.7	1.1	11.8	1.2	11.8	1.2	11.8	1.1	11.8	1.2
BS1102	Erratic	10.6	0.7	10.7	0.8	10.7	0.7	10.7	0.7	10.7	0.8
BS1103	Erratic	10.2	0.7	10.2	0.7	10.2	0.7	10.3	0.7	10.3	0.8
BS1104	Bedrock	13.4	0.9	13.5	1.0	13.5	1.0	13.6	0.9	13.6	1.0
BS1105	Erratic	9.9	0.7	10.0	0.7	10.0	0.7	10.1	0.7	10.1	0.7
BS1106	Bedrock	20.5	1.3	20.6	1.3	20.5	1.3	20.7	1.2	20.7	1.4
BS1107	Erratic	10.8	0.8	10.9	0.8	10.9	0.8	10.8	0.7	10.8	0.8
BS1108	Erratic	10.6	0.7	10.6	0.7	10.6	0.7	10.5	0.6	10.5	0.7
BS1109	Bedrock	10.7	0.7	10.7	0.8	10.7	0.7	10.7	0.7	10.7	0.8
BS1110	Erratic	9.8	0.7	9.8	0.7	9.8	0.7	9.9	0.7	9.9	0.7
BS1111	Erratic	10.5	0.7	10.5	0.7	10.6	0.7	10.6	0.7	10.6	0.8
BS1112	Bedrock	10.1	0.6	10.1	0.7	10.1	0.6	10.2	0.6	10.2	0.7
BS1113	Erratic	11.0	0.6	11.1	0.7	11.1	0.7	11.1	0.6	11.1	0.7
BS1114	Bedrock	11.1	0.7	11.1	0.7	11.1	0.7	11.2	0.7	11.2	0.8
BS1115	Erratic	9.6	0.6	9.7	0.6	9.7	0.6	9.7	0.6	9.7	0.7
Erratic Mean		10.3	0.7	10.4	0.7	10.4	0.7	10.4	0.7	10.4	0.7
Bedrock Mean^b		10.9	0.8	10.9	0.8	10.9	0.8	11.0	0.8	11.0	0.9

^a Kangerdlugssuaq Fjord erratic mean excludes KF1021 (see text).

^b Samples BS1104 and BS1106 are suspected to contain inherited ¹⁰Be and are excluded from the bedrock mean (see text).

4.3. Regional summary

The mean of glacial erratic ¹⁰Be ages from Kangerdlugssuaq Fjord, in the north of the SE sector, is 11.8 ± 1.0 ka. Erratics from Sermilik Fjord are younger, returning a mean age of 10.9 ± 0.4 ka. The mean age of erratic samples from Bernstorffs Fjord, in the south of the sector, is 10.4 ± 0.5 ka.

Mean erratic exposure ages from all fjords overlap within 1 standard deviation, however, the distribution of samples suggests they may represent distinct populations (Fig. 6). A t-test (2 tailed, unequal sample variance) comparing erratic samples from Kangerdlugssuaq and Bernstorffs Fjords returns a *P* value of 0.010, demonstrating the populations are statistically distinct (at the 95% confidence interval). Relative probability density ‘camel’ plots (Fig. 4) and box and whisker plots (Fig. 6) further illustrate that erratics from Kangerdlugssuaq Fjord are generally older than those from Bernstorffs Fjord.

Further *t*-tests on samples from Sermilik Fjord (Hughes et al., 2012) show erratic ages from here are separable (at 95%) from those in Bernstorffs Fjord (*P* = 0.049), whilst samples from Kangerdlugssuaq are not (*P* = 0.060).

5. Discussion

The exposure ages reported here significantly extend the spatial coverage of cosmogenic exposure dating in SE Greenland which was previously limited to the area around Sermilik Fjord (Roberts et al., 2008 – Fig. 5; Hughes et al., 2012).

5.1. Timing and mechanisms of fjord deglaciation

Deglaciation occurred first at Kangerdlugssuaq Fjord, in the north of the SE sector, at ~11.8 ka. Further south, deglaciation at

Sermilik and Bernstorffs Fjords occurred later at ~10.9 ka and ~10.4 ka respectively.

Erratic samples from Kangerdlugssuaq Fjord yield a mean exposure age of 11.8 ± 1.0 ka, this is broadly consistent with radiocarbon dates from the inner-continental shelf that frame the onset of terrestrial retreat as sometime after 12.9 cal ka BP (Fig. 5 – Jennings et al., 2006). Sediment cores from the Kangerdlugssuaq Trough and surrounding shelf areas show increased $\delta^{18}\text{O}$ values, high levels of ice-raftered debris (IRD) (Jennings et al., 2006) and peaks of Ash Zone 2 tephra (Jennings et al., 2002a) from ~13 to 11.5 cal ka BP, which are indicative of a significant ice-wasting event during this period.

Exposure ages indicate that Kangerdlugssuaq Fjord deglaciated towards the end of the Younger Dryas stadial (YD) (12.8–11.6 ka – Alley, 2000). At first glance this is perhaps counter-intuitive; the YD is recorded in Greenland ice cores as the coldest event of the last 15 ka, with temperatures 15°C colder than the present-day (Cuffey and Clow, 1997; Seieringhaus et al., 1998; Alley, 2000; Vinther et al., 2008). Furthermore, some glaciers advanced in Greenland during this interval (Alley et al., 2010). Moraines of the Milne Land Stage (MLS) in East Greenland record a significant readvance of both independent glaciers and the GrIS margin and are broadly constrained to the YD (Funder, 1972, 1978; Denton et al., 2005; Kelly et al., 2008; Hall et al., 2008b; Alexanderson and Håkansson, 2014). There is also evidence for a glacial readvance in West Greenland during this interval; Jakobshavn Isbrae briefly readvanced to a position on the outer-shelf (Ó Cofaigh et al., 2013), and the mid-shelf Fiskebanke moraines further south may have formed during a YD readvance (Weidick et al., 2004; Funder et al., 2011).

Although glaciers advanced during the YD, reconstructions in East Greenland demonstrate that glacial advance was limited relative to the magnitude of cooling (e.g. Alley, 2000). This is

Table 3

Regional deglaciation chronology. Terrestrial and marine radiocarbon dates are recalibrated using CALIB 7.0 (Stuiver et al., 2005) and INTCAL13 or MARINE13 (Reimer et al., 2013). ^{10}Be ages are recalculated using the Arctic production rate (Young et al., 2013) and Lal/Stone time-independent scaling (Lal, 1991; Stone, 2000). ^{10}Be ages are calculated using published erosion rates.

Study	Location	Lat. (°N)	Long. (°W)	Elevation (m)	Dating type	Dated material	Sample ID	^{14}C age	^{14}C error	Age (ka)	Error (ka)
Scoresby Sund											
Cremer et al. (2001)	Raffles Sø, Raffles Ø	70.594	-21.534	40	Terr. ^{14}C	Leaves, twigs	UtC-7428	8900	50	10.0	0.2
Funder (1978)	Morten Sø,	70.886	-22.411	48	Terr. ^{14}C	Gyttja	K-916	9630	120	10.9	0.3
Funder (1978)	Hugin Sø	70.768	-24.096	50	Terr. ^{14}C	Gyttja	K-2034	10,050	150	11.7	0.5
Kelly et al. (2008)	Gurreholm Dal, Stauning Alper	71.403	-24.715	129	^{10}Be	Moraine boulders	MKG-15 ^a	—	—	12.3	0.6
Levy et al. (2013)	Bregne ice cap	70.910	-25.595	744	^{10}Be	Erratics and bedrock	Erratic mean	—	—	10.7	0.4
Lowell et al. (2013)	Istorvet ice cap	70.888	-22.264	455	^{10}Be	Erratics	Erratic mean	—	—	11.7	0.6
Nam et al. (1995)	Scoresby Sund trough mouth fan	70.120	-17.710	-1617	Mar. ^{14}C	<i>N. pachyderma</i> (sin.)	Modelled age	—	—	15.8	—
Kangerdlugssuaq											
Andrews et al. (1997)	Outer-Kangerdlugssuaq Trough	66.203	-30.655	-496	Mar. ^{14}C	Mixed foraminifera	AA-4026	13,585	110	15.8	0.4
Andrews et al. (1997)	Mid-Kangerdlugssuaq Trough	66.764	-30.840	-295	Mar. ^{14}C	Mixed foraminifera	AA-6848	14,845	190	17.6	0.5
Andrews et al. (1997)	Mikis Fjord	68.116	-31.432	-244	Mar. ^{14}C	Mixed foraminifera	AA-11584	9975	100	10.9	0.3
Jennings et al. (2002b)	Inner-Nansen Trough	68.100	-29.350	404	Mar. ^{14}C	Mixed foraminifera	CAMS-32047	9800	60	10.8	0.2
Jennings et al. (2006)	Mid-Kangerdlugssuaq Trough	67.288	-30.960	-557	Mar. ^{14}C	<i>Elphidium excavatum</i>	AA-29204	13,830	270	16.2	0.8
Jennings et al. (2006)	Mid-Kangerdlugssuaq Trough	67.300	-30.967	-574	Mar. ^{14}C	<i>Nonionella Labradorica</i>	AA-29205	11,380	80	12.9	0.2
Jennings et al. (2006)	Mid-Kangerdlugssuaq Trough	67.047	-30.860	-668	Mar. ^{14}C	Mixed foraminifera	AA-32045	12,900	50	14.7	0.4
Jennings et al. (2006)	Outer-Kangerdlugssuaq Trough	65.963	-30.633	-478	Mar. ^{14}C	<i>Triloculina</i> sp.	AA-23221	14,550	150	17.2	0.5
Jennings et al. (2006)	Grivel Basin	68.093	-27.836	-556	Mar. ^{14}C	Bryozoans	AA-43116	11,950	110	13.4	0.2
Mienert et al. (1992)	Inner-Kangerdlugssuaq Trough	67.410	-31.066	-624	Mar. ^{14}C	Mixed foraminifera	AA-4666	9375	70	10.2	0.2
This study	Kangerdlugssuaq Fjord head	68.432	-32.335	116	^{10}Be	Erratics	Erratic mean	—	—	11.8	1.0
This study	Kangerdlugssuaq Fjord mouth	68.138	-32.066	178	^{10}Be	Erratics	Erratic mean	—	—	11.8	1.0
Sermilik Fjord											
Hughes et al. (2012)	Sermilik Fjord mouth	65.857	-38.006	112	^{10}Be	Erratics	Erratic mean	—	—	10.9	0.4
Hughes et al. (2012)	Sermilik Fjord head	66.226	-37.593	76	^{10}Be	Erratics	Erratic mean	—	—	10.9	0.4
Jakobsen et al. (2008)	Mittivakkat, Sermilik Fjord	65.692	-37.907	90	Terr. ^{14}C	Clay and gyttja	AAR-1542	9890	110	11.5	0.4
Roberts et al. (2008)	Toqulelertivit Imit Valley	65.757	-38.293	<400	^{10}Be , ^{26}Al	Bedrock	Bedrock mean	—	—	12.4	1.2
Long et al. (2008)	Ammassalik Fjord	65.754	-37.271	97	Terr. ^{14}C	Gyttja (bulk sample)	SUERC-9428	9659	67	11.0	0.2
Bernstorffs Fjord											
Kuijpers et al. (2003)	Continental slope	63.042	-38.659	-1843	Mar. ^{14}C	<i>N. pachyderma</i> (sin.)	AAR 5044	13,700	100	16.0	0.3
Kuijpers et al. (2003)	Mid-continental shelf	63.523	-39.713	-620	Mar. ^{14}C	<i>Nonionella Labradorica</i>	AAR 4034-2	12,930	140	14.7	0.5
This study	Bernstorffs Fjord mouth	63.668	-40.771	111	^{10}Be	Erratics	Erratic mean	—	—	10.4	0.7
This study	Mid-Bernstorffs Fjord	63.725	-41.214	237	^{10}Be	Erratics	Erratic mean	—	—	10.4	0.7
Kap Farvel											
Bennike et al. (2002)	Lake N14, Angissøq, Nanortalik	59.980	-45.179	33	Terr. ^{14}C	Marine algae	Ua-14845	11,995	130	13.9	0.3
Larsen et al. (2011)	Lower Nordbosø, Narssarssuaq	61.344	-45.367	600	Terr. ^{14}C	Gyttja (bulk sample)	LuS8724	9490	65	10.8	0.3

^a Youngest of GII moraine.

attributed to enhanced seasonality; the YD was characterised by very cold winters and moderately cool summers (Denton et al., 2005; Kelly et al., 2008; Hall et al., 2008b). Proxy climate data from southern Greenland are consistent with this, recording mild summers and cold, arid winters during this interval (Björck et al., 2002). Glaciers in East Greenland may have retreated towards the end of the YD, perhaps in response to slight warming (Kelly et al., 2008; Hall et al., 2010). There is also convincing evidence for pervasive deglaciation in parts of West Greenland throughout the YD. Ice retreated rapidly from the continental shelf north of Disko Bugt (Ó Cofaigh et al., 2013) before ‘collapsing’ ~100 km through the Uummannaq Fjord system by 11.4–10.8 ka (Roberts et al., 2013). The driving mechanism of retreat in West Greenland remains unclear. Despite enhanced seasonality, climate in Baffin Bay remained 4–5°C colder than at present (Young et al., 2012). Both intermediate and surface ocean temperatures were cold in Baffin Bay during the YD; annual sea ice cover of 9–11 months is reconstructed from dinoflagellate assemblages (Jennings et al., 2014) and warm Atlantic water was not present in Disko Bugt until ~9.2 cal ka BP (Lloyd et al., 2005).

The strong coherence of climate records from across Greenland (e.g. Johnsen et al., 2001; Vinther et al., 2008) indicates a uniform regional cooling during the YD. In contrast, reconstructions based on foraminiferal assemblage data show that oceanic conditions in the SE region were drastically different to West Greenland during this interval. Cores from Kangerdlugssuaq Trough show high

percentages of *Cassidulina neoteretis* during the YD (Jennings et al., 2006 – Fig. 6). *C. neoteretis* is associated with modified warm Atlantic waters (e.g. Jennings and Helgadóttir, 1994; Duplessy et al., 2001; Andresen et al., 2013). Peaks in $\delta^{13}\text{C}$ values on the inner-shelf at ~12.8 cal ka BP are attributed to methane clathrate expulsion events; these occur during sediment warming and pressure release (Smith et al., 2001) and are consistent with foraminiferal data. We suggest that the incursion of warm water into Kangerdlugssuaq Trough during the YD overrode the climatic signal and triggered the deglaciation of Kangerdlugssuaq Fjord.

Despite the recent application of cosmogenic isotope dating (this study, Roberts et al., 2008; Hughes et al., 2012), the behaviour of the GrIS in SE Greenland during the YD remains enigmatic. A constructional feature on a prominent bedrock ridge in Kangerdlugssuaq Trough (Stein, 1996; Fig. 5 – Andrews et al., 1997) may be a YD moraine, but unfortunately the age of this feature is not well-constrained. Terrestrial and marine dates from across the sector indicate the ice margin was on the inner-continental shelf during the early YD (Fig. 5) but we are unable to establish whether there was a regional readvance event during this interval. High-resolution sediment cores and detailed bathymetric mapping may help resolve this.

Exposure ages from erratics in Bernstorffs Fjord indicate the onset of terrestrial deglaciation at around 10.4 ka; slightly later than retreat in Sermilik Fjord and substantially later than the

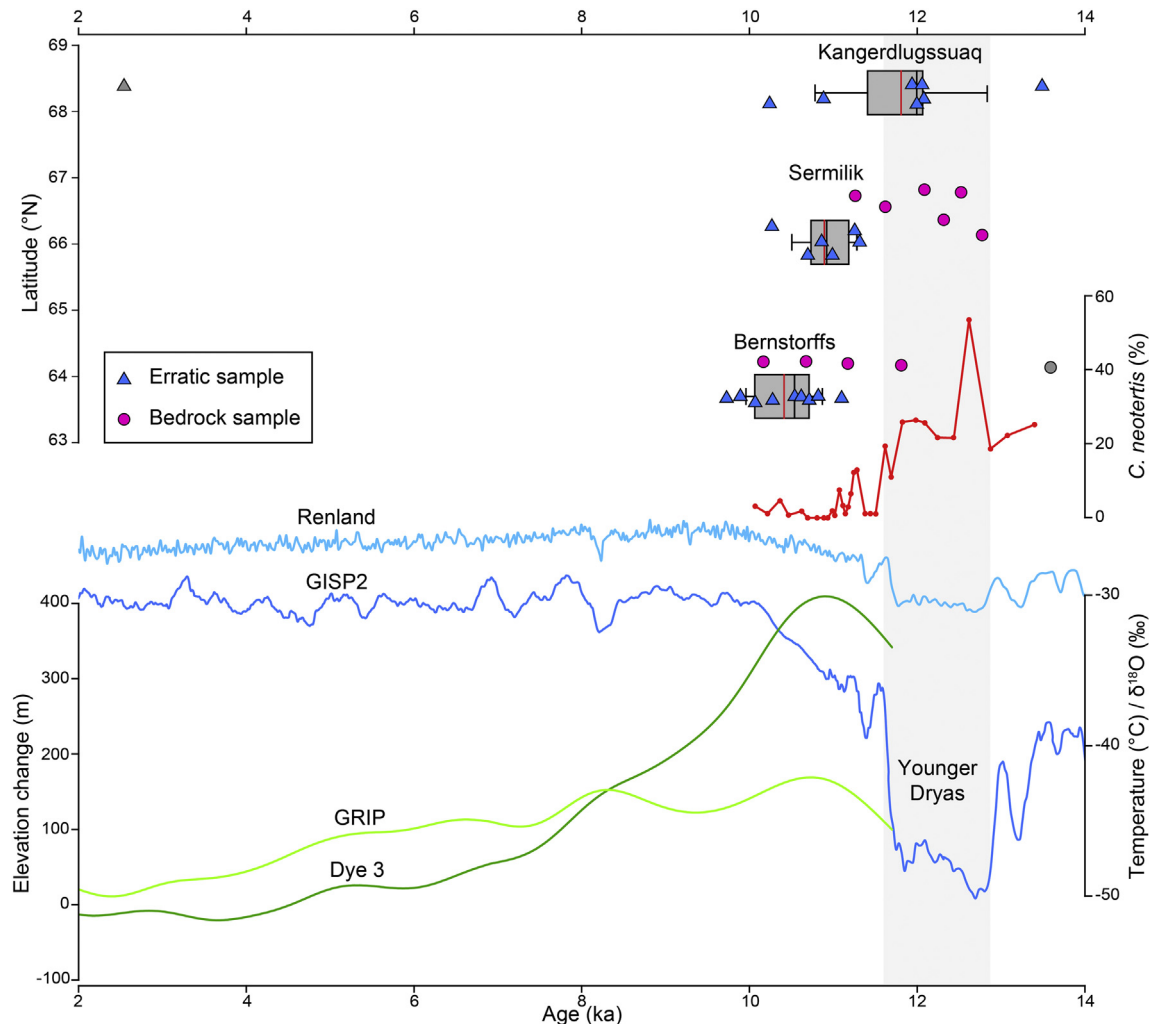


Fig. 6. Regional ^{10}Be exposure ages with climate and ice sheet proxies. Boxes show first and third quartiles with median. Whiskers show 1σ around mean (red). Red line shows % of *Cassidulina neotertis* from core JM96-1216/2-GC in Kangerdlugssuaq Trough, a proxy for incursion of modified Atlantic water (i.e. the IC – Jennings et al., 2006). GISP2 ice surface temperatures derived from $\delta^{18}\text{O}$ measurements (Cuffey and Clow, 1997; Alley, 2000). Renland $\delta^{18}\text{O}$ record from Vinther et al. (2008). Ice sheet surface elevation changes at Dye 3 and GRIP are plotted from Vinther et al. (2009). Bedrock samples are displaced 0.5°N for clarity. Bedrock sample BS1106 (20.7 ± 1.2 ka) is not plotted. (For interpretation of the references to colour in this figure legend, the reader is referred to the web version of this article.)

deglaciation of Kangerdlugssuaq Fjord. A paucity of terrestrial and oceanic proxy data from the south of the SE sector (see Fig. 5) makes verifying the timing of deglaciation from independent evidence challenging. The onset of ice-sheet thinning at Dye 3, ~170 km north-west of Bernstorffs Fjord, just before 10 ka (Fig. 6) probably reflects dynamic thinning (e.g. Pritchard et al., 2009) triggered by ice retreat and is consistent with fjord deglaciation during this interval. The tight grouping of exposure ages from Bernstorffs Fjord ($\sigma = 456$ yr) also suggests samples accurately reflect glacier retreat (Fig. 6). The deglaciation of Sermilik and Bernstorffs Fjords occurred during a period of dramatic climate amelioration (Fig. 6), we support the hypothesis of Hughes et al. (2012) and suggest that retreat in these fjords occurred in response to rapidly warming climate following the termination of the YD.

5.2. Regional timing of deglaciation

Kangerdlugssuaq Fjord, in the north of the SE sector, deglaciated prior to both Sermilik and Bernstorffs Fjords in the centre and south of the sector. Variation in the timing of fjord deglaciation suggests

that retreat was paced by local factors, rather than directly by regional-scale forcing mechanisms (i.e. climate or ocean conditions).

We propose that deglaciation in Kangerdlugssuaq Fjord was initiated by the incursion of the warm IC onto the continental shelf through Kangerdlugssuaq Trough (cf. Holland et al., 2008; Murray et al., 2010; Straneo et al., 2010). The delay in deglaciation between Kangerdlugssuaq Glacier and glaciers further south implies that the centre and south of the sector were subject to different conditions during the YD. Either warm IC water did not penetrate transverse trough systems further south or, alternatively, it had a diminished impact on glacier behaviour. Warm IC water flows at depth on the continental shelf beneath cold, fresh Arctic water masses (Straneo et al., 2010; Brearley et al., 2012; Sutherland et al., 2013 – see Section 2). We suggest that the influence of the IC was minimised by complex shelf bathymetry off Sermilik Fjord (Straneo et al., 2010; Schjøth et al., 2012; Sutherland and Straneo, 2012; Inall et al., 2014) and by a shallow sill (~250 m bsl) at the mouth of Bernstorffs Fjord (unpublished GLIMPSE cruise data, 2011). We propose that bathymetric constrictions off both fjord systems weakened or prevented IC water from influencing the ice margin,

thereby buffering it from retreat until dramatic climatic amelioration during the early Holocene. In contrast, Kangerdlugssuaq Fjord has a well-developed, deep trough which extends ~250 km to the shelf-break (Fig. 1). Consequently, Kangerdlugssuaq Glacier was directly influenced by the incursion of warm IC water during the YD. Modern oceanographic conditions may provide an analogue for this hypothesis: IC heat delivery to Kangerdlugssuaq Fjord is an order of magnitude larger than at Sermilik Fjord (Sutherland and Straneo, 2012; Inall et al., 2014). This may simply reflect ephemeral oceanic conditions during sampling (Inall et al., 2014), however, it is considered more likely that IC heat delivery in Sermilik Fjord is limited by constricted shelf bathymetry or cold ocean current barriers (Sutherland et al., 2013).

The effect of the IC on glaciers in the south of the sector may also have been muted by mixing and cooling with cold Polar water of the EGC and EGCC during southerly advection along the continental margin. Analysis of oceanographic measurements suggests that IC core waters cool by ~1°C and freshen during transit around the Irminger Basin (Goldsack, 2013). We suggest downstream cooling of the IC was probably further enhanced during deglaciation by large volumes of meltwater from the GrIS (e.g. Smith et al., 2001; Jennings et al., 2002a). Reconstructions of oceanic conditions in the south of the region through the YD and early Holocene are required to fully assess the relative importance of oceanic and climatic forcing on deglaciation across the SE sector.

Glacial retreat at Bernstorffs Fjord (10.4 ± 0.5) and Sermilik Fjord (10.9 ± 0.4) occurred later than at Kangerdlugssuaq Fjord during a period of dramatic climatic warming (Fig. 6). The mean of erratic exposure ages from Bernstorffs and Sermilik Fjords overlap within 1σ , but a *t*-test ($P = 0.049$) demonstrates populations are separable. We suggest that the slight delay in the timing of deglaciation at Bernstorffs Fjord relative to Sermilik Fjord may stem from the more prominent bathymetric shallowing at the mouth of Bernstorffs Fjord (unpublished GLIMPSE cruise data, 2011). Bernstorffs Glacier may have remained pinned in a stable configuration at the mouth of the fjord during initial climate amelioration.

Given the close timing of deglaciation in Sermilik and Bernstorffs Fjords we consider it likely that marine-terminating outlet glaciers with similar bathymetry in the centre and south of the sector also retreated in response to climatic amelioration following the termination of the YD (Fig. 5).

5.3. Fjord deglaciation style

Exposure ages from fjord axis transects from across the region demonstrate that, regardless of timing, once retreat was initiated, it was rapid and persistent in all locations. This is consistent with geomorphological observations and detailed bathymetric data which show no evidence for stillstand or readvance events (Brooks, 1979; Andrews et al., 1994; Dowdeswell et al., 2010; Hughes et al., 2012). Retreat was continuous despite the presence of Ensomheden Island in Bernstorffs Fjord and significant narrowing, bathymetric shallowing and a large island (Depot Ø) in Sermilik Fjord (Hughes et al., 2012). Average retreat rates from across the region vary from ~10 m a⁻¹ to ~80 m a⁻¹ and probably represent minimum estimates; fjord systems may have deglaciated over timescales as short as several hundred years. Transects do not cover the full length of the fjord systems but retreat likely continued to within present-day ice margins, only stabilising once glaciers had retreated into shallow tidewater or terrestrial settings (e.g. Hughes et al., 2012).

Rapid retreat through fjord systems may simply reflect the continuing influence of forcing mechanisms that triggered deglaciation (i.e. ocean/climate warming – see above). Alternatively, outlet glacier retreat through deep fjord systems may be, at least

partially, decoupled from climatic and oceanic forcing. We favour the latter and suggest that in the large, deep fjords of SE Greenland retreat was primarily paced by the interplay between internal glacier dynamics and fjord geometry (e.g. Larsen et al., 2013). Rapid deglaciation is sustained by dynamic mechanisms; initial margin retreat results in increased surface slope and drives glacier acceleration. In turn, this causes dynamic thinning, which promotes buoyancy-driven calving and further margin retreat (Meier and Post, 1987; Howat et al., 2005; Joughin et al., 2008).

Although we do not have samples to directly constrain glacier thinning, our data demonstrate the rapid retreat of glaciers in large fjord systems which is intrinsically linked to fast-paced thinning. We apply modern centreline gradients from Bernstorffs and Kangerdlugssuaq Glaciers (Howat et al., 2014) to approximate glacier thickness when the glacier terminus was at the mouth of each fjord. During fjord deglaciation we tentatively estimate that thinning of >1000 m occurred at the head of both Kangerdlugssuaq and Bernstorffs Fjords. There are obvious limitations in assuming that modern geometry is applicable to an extended GrIS configuration, not least because the beds of the fjord systems are much deeper than the bed inland of the present-day margin (Dowdeswell et al., 2010; Bamber et al., 2013; unpublished GLIMPSE cruise data, 2011). Nonetheless, these estimates are broadly reconcilable with observations of ice-scoured terrain to at least 1000 m asl in Bernstorffs Fjord and glacially scoured terrain and perched erratics to at least 1200 m asl in Kangerdlugssuaq Fjord (Brooks, 1979).

5.4. Implications for Holocene glacier behaviour

Geomorphological observations and ¹⁰Be exposure ages from Kangerdlugssuaq and Bernstorffs Fjords show no evidence for glacier readvance until the late Holocene. This contrasts with West Greenland and Baffin Island where glaciers advanced during the 9.3 and 8.2 ka events (Briner et al., 2009; Young et al., 2011a,b, 2012). We suggest that the effect of these cold events on marine-terminating glaciers in SE Greenland may have been tempered by the influence of warm oceanographic conditions at the time (Andersen et al., 2004; Jennings et al., 2006, 2011). However, it is also possible that glaciers in SE Greenland did advance in response to cooling, but from a position well inboard of the present-day ice margin, and thus evidence is not preserved (Kelly et al., 2008).

Kangerdlugssuaq and Bernstorffs Glaciers probably achieved their maximum Holocene extents during the LIA, similar to Helheim Glacier at the head of Sermilik Fjord (Hughes et al., 2012). Photos taken in 1930 (Wager et al., 1937) and an early map (Spender, 1933) show Kangerdlugssuaq Glacier close to a prominent lateral moraine at the head of the fjord; this is assumed to be of LIA age. A large submarine ridge here is thought to be the extension of the LIA moraine (Syvitski et al., 1996). Aerial photos from Bernstorffs Fjord taken in the 1930s confirm a similar situation in the south of the sector; Bernstorffs Glacier was within 500 m of well-defined trimlines thought to represent the maximum LIA position (A. Bjørk, personal communication).

5.5. Isotopic inheritance in bedrock

The mean age of bedrock samples from Bernstorffs Fjord is older (~11.0 ka) than the mean of accompanying erratic samples (~10.4 ka). This is also observed in Sermilik Fjord where bedrock samples are on average ~1.2 ka older than their erratic counterparts (Hughes et al., 2012). Although bedrock and erratic samples overlap within uncertainties, the near-consistent offset between the two suggests a systematic cause rather than inherent sample variability. Bedrock samples are thought to exhibit a minor degree of isotopic inheritance from previous periods of exposure. This contrasts with

comparable low-elevation sites in West Greenland where bedrock samples appear to accurately track the timing of deglaciation (Corbett et al., 2011; Kelley et al., 2013; Larsen et al., 2013; Roberts et al., 2013; Young et al., 2013).

Nuclide inheritance may simply reflect insufficient erosion (i.e. <2 m – Gosse and Phillips, 2001) through MIS 2. Whilst this might be expected at passive margins, it is considered less likely in these large fjord systems which hosted fast, highly erosive ice streams during MIS 2 (e.g. Dowdeswell et al., 2010; Hughes et al., 2012). Alternatively, bedrock inheritance may reflect rapid oscillations of the ice margin. This interpretation is hindered by the absence of geomorphic evidence for corresponding stillstand or readvance events across the SE region (e.g. Brooks, 1979; Andrews et al., 1994; Hughes et al., 2012; unpublished GLIMPSE cruise data, 2011). It is possible that fjord systems deglaciated before experiencing brief, full-fjord readvances, followed by final retreat. The provenance of inherited ^{10}Be remains unresolved and warrants further investigation.

6. Conclusions

Exposure ages reported here significantly extend the spatial coverage of cosmogenic isotope dating in SE Greenland which was previously limited to the area around Sermilik Fjord in the centre of the sector (Roberts et al., 2008; Hughes et al., 2012). These new age determinations track the deglaciation of large, high-discharge outlet glaciers of the GrIS and permit examination of the timing and style of retreat across the SE region.

- Kangerdlugssuaq Fjord in the north of the SE sector deglaciated at ~11.8 ka during the late YD, retreat was primarily driven by the incursion of warm IC waters during cool climatic conditions.
- Bernstorffs Fjord deglaciated later at ~10.4 ka, broadly coincident with retreat at Sermilik Fjord at ~10.9 ka (Hughes et al., 2012); retreat was driven by rapid climatic amelioration at the start of the Holocene.
- Deglaciation of Kangerdlugssuaq Fjord preceded glaciers further to the south by ~1 ka. We attribute this behaviour to the variation in the influence of the IC on the ice margin which appears to be mediated by the offshore bathymetry of individual fjord systems.
- Once initiated, ice retreat was rapid and continuous in all fjord settings despite shoaling and obstacles to ice flow. Retreat likely continued within present-day ice margins, stabilising only when glaciers reached shallow marine or terrestrial settings. Rapid glacier retreat was accompanied by fast-paced thinning.
- New ^{10}Be exposure ages and geomorphological observations from major fjord systems across SE Greenland show no evidence for Holocene readvance events prior to the LIA.

Acknowledgements

We are grateful for insightful comments from Nicolás Young and an anonymous reviewer which improved this manuscript. Laurence Dyke is funded by a NERC CASE doctoral scholarship (NE/I528126/1). Fieldwork was supported by the Leverhulme Trust (Murray; GLIMPSE Project) and the National Geographic Society (Project No. 111741). We thank the captain (Sigurður Petturson) and crew of M/V *þýtur*. Robert Peroni provided logistical support in Greenland. Kilian Scharrer and Nick Selmes assisted with sample collection. 23 ^{10}Be exposure ages were funded by the Natural Environment Research Council (NERC) Cosmogenic Isotope Analysis Facility (CIAF, 9098.1010 and 9113.1011). Sample preparation was undertaken at the Paleoclimate Laboratory, University at Buffalo under the supervision of Jason Briner and Nicolás Young. Additional

processing was undertaken at Camborne School of Mines and at the NERC CIAF. We thank Allan Davidson and Delia Gheorghiu for assistance with mineral separation and final sample preparation. AMS measurements were undertaken by Dylan Rood and Sheng Xu. We thank Anders Bjørk for enlightening discussions on the LIA in SE Greenland.

References

- Aagaard, K., Coachman, L.K., 1968a. The East Greenland Current north of Denmark Strait: part I. Arctic 21, 181–200.
- Aagaard, K., Coachman, L.K., 1968b. The East Greenland Current north of Denmark Strait: part II. Arctic 21, 267–290.
- Alexander, H., Häkansson, L., 2014. Coastal glaciers advanced onto Jameson Land, East Greenland during the late glacial-early Holocene Milne Land Stade. *Polar Research* 33.
- Alley, R., 2000. The Younger Dryas cold interval as viewed from central Greenland. *Quaternary Science Reviews* 19 (1–5), 213–226.
- Alley, R.B., Andrews, J.T., Brigham-Grette, J., Clarke, G.K.C., Cuffey, K.M., Fitzpatrick, J.J., Funder, S., Marshall, S.J., Miller, G.H., Mitrovica, J.X., Muhs, D.R., Otto-Bliesner, B.L., Polyak, L., White, J.W.C., 2010. History of the Greenland Ice Sheet: paleoclimatic insights. *Quaternary Science Reviews* 29 (15–16), 1728–1756.
- Andersen, C., Koč, N., Jennings, A., Andrews, J.T., 2004. Nonuniform response of the major surface currents in the Nordic Seas to insolation forcing: implications for the Holocene climate variability. *Paleoceanography* 19 (2), 1–16.
- Andresen, C.S., Hansen, M.J., Seidenkrantz, M.-S., Jennings, A.E., Knudsen, M.F., Nørgaard-Pedersen, N., Larsen, N.K., Kuijpers, A., Pearce, C., 2013. Mid- to late-Holocene oceanographic variability on the Southeast Greenland shelf. *The Holocene* 23, 167–178.
- Andrews, J.T., Jennings, A.E., Cooper, T., Williams, K.M., Mienert, J., 1996. Late Quaternary sedimentation along a fjord to shelf (trough) transect, East Greenland (c. 68°N). In: Late Quaternary Oceanography of North Atlantic Margins. Vol. Special Publication II. Geological Society of London, pp. 153–166.
- Andrews, J.T., Milliman, J.D., Jennings, A.E., Rynes, N., Dwyer, J., November 1994. Sediment thicknesses and Holocene Glacial marine sedimentation rates in three East Greenland Fjords (ca. 68°N). *Journal of Geology* 102 (6), 669–683.
- Andrews, J.T., Smith, L.M., Preston, R., Cooper, T., Jennings, A.E., January 1997. Spatial and temporal patterns of iceberg rafting (IRD) along the East Greenland margin, ca. 68°N, over the last 14 cal ka. *Journal of Quaternary Science* 12, 1–13.
- Bacon, S., Reverdin, G., Rigor, I.G., Snaith, H.M., 2002. A freshwater jet on the east Greenland shelf. *Journal of Geophysical Research: Oceans* 107 (C7), 1–16.
- Balco, G., 2011. Contributions and unrealized potential contributions of cosmogenic-nuclide exposure dating to glacier chronology, 1990–2010. *Quaternary Science Reviews* 30 (1–2), 3–27.
- Balco, G., Briner, J.P., Finkel, R.C., Rayburn, J.A., Ridge, J.C., Schaefer, J.M., 2009. Regional beryllium-10 production rate calibration for late-glacial northeastern North America. *Quaternary Geochronology* 4 (2), 93–107.
- Bales, R.C., Guo, Q., Shen, D., McConnell, J.R., Du, G., Burkhardt, J.F., Spikes, V.B., Hanna, E., Cappelen, J., Mar 2009. Annual accumulation for Greenland updated using ice core data developed during 2000–2006 and analysis of daily coastal meteorological data. *Journal of Geophysical Research: Atmospheres* 114 (D13), D06116.
- Bamber, J.L., Griggs, J.A., Hurkmans, R.T.W.L., Dowdeswell, J.A., Gogineni, S.P., Howat, I., Mouginot, J., Paden, J., Palmer, S., Rignot, E., Steinhage, D., 2013. A new bed elevation dataset for Greenland. *The Cryosphere* 7 (2), 499–510.
- Bennike, O., 2002. Late Quaternary history of Washington Land, North Greenland. *Boreas* 31 (3), 260–272.
- Bennike, O., Björck, S., Lambeck, K., 2002. Estimates of South Greenland late-glacial ice limits from a new relative sea level curve. *Earth and Planetary Science Letters* 197, 171–186.
- Björck, S., Bennike, O., Ingólfsson, O., Barnekow, L., Penney, D.N., 1994. Lake Bokshandsken's earliest postglacial sediments and their palaeoenvironmental implications, Jameson Land, East Greenland. *Boreas* 23 (4), 459–472.
- Björck, S., Bennike, O., Rosén, P., Andresen, C.S., Bohncke, S., Kaas, E., Conley, D., 2002. Anomalously mild Younger Dryas summer conditions in southern Greenland. *Geology* 30 (5), 427–430.
- Brearley, J.A., Pickart, R.S., Valdimarsson, H., Jonsson, S., Schmitt, R.S.W., Haine, T.W.N., 2012. The East Greenland boundary current system south of Denmark Strait. *Deep Sea Research Part I: Oceanographic Research Papers* 63, 1–19.
- Briner, J.P., Bini, A.C., Anderson, R.S., 2009. Rapid early Holocene retreat of a Laurentide outlet glacier through an Arctic Fjord. *Nature Geoscience* 2, 496–499.
- Briner, J.P., Miller, G.H., Finkel, R.C., Hess, D.P., 2008. Glacial erosion at the fjord onset zone and implications for the organization of ice flow on Baffin Island, Arctic Canada. *Geomorphology* 97 (1–2), 126–134.
- Brooks, C.K., 1979. Geomorphological observations at Kangerdlugssuaq, East Greenland. *Meddelelser om Grönland* 1, 1–21.
- Carlson, A.E., Stoner, J.S., Donnelly, J.P., Hillaire-Marcel, C., May 2008. Response of the southern Greenland Ice Sheet during the last two deglaciations. *Geology* 36 (5), 359–362.
- Child, D., Elliott, G., Mifsud, C., Smith, A.M., Fink, D., 2000. Sample processing for earth science studies at ANTARES. *Nuclear Instruments and Methods in Physics Research Section B: Beam Interactions with Materials and Atoms* 172 (1), 856–860.

- Christoffersen, P., O'Leary, M., van Angelen, J.H., van den Broeke, M., 2012. Partitioning effects from ocean and atmosphere on the calving stability of Kangerdlugssuaq Glacier, East Greenland. *Annals of Glaciology* 53 (60), 249–256.
- Corbett, L.B., Young, N.E., Bierman, P.R., Briner, J.P., Neumann, T.A., Rood, D.H., Graly, J.A., 2011. Paired bedrock and boulder ^{10}Be concentrations resulting from early Holocene ice retreat near Jakobshavn Isfjord, western Greenland. *Quaternary Science Reviews* 30 (13–14), 1739–1749.
- Cremer, H., Wagner, B., Melles, M., Hubberten, H.-W., 2001. The postglacial environmental development of Raffles Sø, East Greenland: inferences from a 10,000 year diatom record. *Journal of Paleolimnology* 26, 67–87.
- Cuffey, K.M., Clow, G.D., November 1997. Temperature, accumulation, and ice sheet elevation in central Greenland through the last deglacial transition. *Journal of Geophysical Research* 102, 26,383–26,396.
- Dawes, P.R., 2009. The bedrock geology under the Inland Ice: the next major challenge for Greenland mapping. *Geological Survey of Denmark and Greenland Bulletin* 17, 57–60.
- Denton, G.H., Alley, R.B., Comer, G.C., Broecker, W.S., 2005. The role of seasonality in abrupt climate change. *Quaternary Science Reviews* 24 (10–11), 1159–1182.
- Desilets, D., Zreda, M., 2003. Spatial and temporal distribution of secondary cosmic-ray nucleon intensities and applications to *in situ* cosmogenic dating. *Earth and Planetary Science Letters* 206 (1–2), 21–42.
- Desilets, D., Zreda, M., Prabu, T., 2006. Extended scaling factors for *in situ* cosmogenic nuclides: new measurements at low latitude. *Earth and Planetary Science Letters* 246 (3–4), 265–276.
- Dowdeswell, J.A., Evans, J., Ó Cofaigh, C., 2010. Submarine landforms and shallow acoustic stratigraphy of a 400 km-long fjord-shelf-slope transect, Kangerlussuaq margin, East Greenland. *Quaternary Science Reviews* 29 (25–26), 3359–3369.
- Dunai, T.J., 2001. Influence of secular variation of the geomagnetic field on production rates of *in situ* produced cosmogenic nuclides. *Earth and Planetary Science Letters* 193 (1–2), 197–212.
- Duplessy, J.-C., Ivanova, E., Murdmaa, I., Paterne, M., Labeyrie, L., 2001. Holocene paleoceanography of the northern Barents Sea and variations of the northward heat transport by the Atlantic Ocean. *Boreas* 30 (1), 2–16.
- Dwyer, J.L., 1995. Mapping tidewater glacier dynamics in East Greenland using Landsat data. *Journal of Glaciology* 41 (139), 584–595.
- Fristrup, B., 1970. Ny geografisk station i Grönland. *Geografisk Tidsskrift* 69 (2), 192–198.
- Funder, S., 1972. Deglaciation of the Scoresby Sund Fjord Region, North-East Greenland. In: Institute Of British Geographers, Special Publications 4, pp. 33–42.
- Funder, S., 1978. Holocene stratigraphy and vegetation history in the Scoresby Sund area, East Greenland. *Bulletin Grönlands Geologiske Undersøgelse* 129, 1–66.
- Funder, S.V., Kjeldsen, K.K., Kjær, K.H., Ó Cofaigh, C., 2011. The Greenland Ice Sheet during the past 300,000 years: A review. In: Ehlers, J., P.L., G., Hughes, P. (Eds.), *Development in Quaternary Sciences: Quaternary Glaciations – Extent and Chronology*, vol. 15. Elsevier, Amsterdam.
- Goldsack, A.E., 2013. Oceanographic Controls on Glaciers in Southeast Greenland (Ph.D. thesis). Swansea University.
- Gosse, J.C., Phillips, F.M., 2001. Terrestrial *in situ* cosmogenic nuclides: theory and application. *Quaternary Science Reviews* 20 (14), 1475–1560.
- Håkansson, L., Alexanderson, H., Hjort, C., Möller, P., Briner, J.P., Aldahan, A., Possnert, G., 2009. Late Pleistocene glacial history of Jameson Land, central East Greenland, derived from cosmogenic ^{10}Be and ^{26}Al exposure dating. *Boreas* 38 (2), 244–260.
- Håkansson, L., Briner, J., Alexanderson, H., Aldahan, A., Possnert, G., 2007. ^{10}Be ages from central east Greenland constrain the extent of the Greenland ice sheet during the Last Glacial Maximum. *Quaternary Science Reviews* 26 (19–21), 2316–2321.
- Håkansson, L., Briner, J.P., Aldahan, A., Possnert, G., 2011. ^{10}Be data from meltwater channels suggest that Jameson Land, east Greenland, was ice-covered during the last glacial maximum. *Quaternary Research* 76 (3), 452–459.
- Hall, B., Baroni, C., Denton, G., Kelly, M.A., Lowell, T., 2008a. Relative sea-level change, Kjøve Land, Scoresby Sund, East Greenland: implications for seasonality in Younger Dryas time. *Quaternary Science Reviews* 27 (25–26), 2283–2291.
- Hall, B.L., Baroni, C., Denton, G.H., 2008b. The most extensive Holocene advance in the Stauning Alper, East Greenland, occurred in the Little Ice Age. *Polar Research* 27 (2), 128–134.
- Hall, B.L., Baroni, C., Denton, G.H., 2010. Relative sea-level changes, Schuchert Dal, East Greenland, with implications for ice extent in late-glacial and Holocene times. *Quaternary Science Reviews* 29 (25–26), 3370–3378.
- Harrower, M., Brewer, C.A., 2003. ColorBrewer.org: an online tool for selecting colour schemes for maps. *The Cartographic Journal* 40 (1), 27–37.
- Hasholt, B., 2000. Evidence of a warmer climate around AD 600, Mittivakkat Glacier, South East Greenland. *Geografisk Tidsskrift* 100, 88–90.
- Hastings Jr., A.D., October 1960. Environment of Southeast Greenland. Tech. Rep. EP-140. Quartermaster Research and Engineering Center, Environmental Protection Research Division, Natick, Massachusetts.
- Hátún, H., Sandø, A.B., Drange, H., Hansen, B., Valdimarsson, H., 2005. Influence of the Atlantic Subpolar Gyre on the thermohaline circulation. *Science* 309 (5742), 1841–1844.
- Henriksen, N., Higgins, A.K., Kalsbeek, F., Pulvertaft, T.C.R., 2000. Greenland from Archaean to Quaternary. Descriptive text to the Geological map of Greenland, 1: 2,500,000. *Geology of Greenland Survey Bulletin* 185, 1–93.
- Holland, D.M., Thomas, R.H., de Young, B., Ribergaard, M.H., Lyberth, B., 2008. Acceleration of Jakobshavn Isbrae triggered by warm subsurface ocean waters. *Nature Geoscience* 1, 659–664.
- Howat, I.M., Joughin, I., Fahnestock, M., Smith, B.E., Scambos, T.A., 2008. Synchronous retreat and acceleration of southeast Greenland outlet glaciers 2000–06: ice dynamics and coupling to climate. *Journal of Glaciology* 54 (187), 646–660.
- Howat, I.M., Joughin, I., Tulaczyk, S., Gogineni, S., Nov. 2005. Rapid retreat and acceleration of Helheim Glacier, east Greenland. *Geophysical Research Letters* 32, L22502.
- Howat, I.M., Negrete, A., Smith, B.E., 2014. The Greenland Ice Mapping Project (GIMP) land classification and surface elevation datasets. *The Cryosphere Discussions* 8 (1), 453–478.
- Hughes, A.L.C., Rainsley, E., Murray, T., Fogwill, C.J., Schnabel, C., Xu, S., 2012. Rapid response of Helheim Glacier, southeast Greenland, to early Holocene climate warming. *Geology* 40 (5), 427–430.
- Humlum, O., Christiansen, H.H., 2008. Geomorphology of the Ammassalik Island, SE Greenland. *Geografisk Tidsskrift* 108 (1), 5–20.
- Inall, M.E., Murray, T., Cottier, F.R., Scharrer, K., Boyd, T.J., Heywood, K.J., Bevan, S.L., 2014. Oceanic heat delivery via Kangerlussuaq Fjord to the south-east Greenland ice sheet. *Journal of Geophysical Research: Oceans* 119 (2), 631–645.
- IOC, IHO, BODC, 2003. Centenary Edition of the GEBCO Digital Atlas. Intergovernmental Oceanographic Commission and the International Hydrographic Organization as part of the General Bathymetric Chart of the Oceans; British Oceanographic Data Centre, Liverpool.
- Iverson, T., 1936. Sydøstgrönland Jan Mayen fiskerundersøkelser. Tech. Rep. 1. Norwegian Directorate of Fisheries.
- Jakobsen, B.H., Fredskild, B., Torp Pedersen, J.B., 2008. Holocene changes in climate and vegetation in the Ammassalik area, East Greenland, recorded in lake sediments and soil profiles. *Geografisk Tidsskrift* 108 (1), 21–50.
- Jakobsson, M., Mayer, L., Coakley, B., Dowdeswell, J.A., Forbes, S., Friedman, B., Hodnesdal, H., Noormets, R., Pedersen, R., Rebesco, M., Schenke, H.W., Zarayskaya, Y., Accettella, D., Armstrong, A., Anderson, R.M., Biehoff, P., Camerlenghi, A., Church, I., Edwards, M., Gardner, J.V., Hall, J.K., Hell, B., Hestvik, O., Kristoffersen, Y., Marcussen, C., Mohammad, R., Mosher, D., Nghiem, S.V., Pedrosa, M.T., Travagliini, P.G., Weatherall, P., 2012. The International Bathymetric Chart of the Arctic Ocean (IBCAO) version 3.0. *Geophysical Research Letters* 39 (L12609), L12609.
- Jennings, A., Andrews, J., Wilson, L., 2011. Holocene environmental evolution of the SE Greenland Shelf North and South of the Denmark Strait: Irminger and East Greenland current interactions. *Quaternary Science Reviews* 30 (7–8), 980–998.
- Jennings, A.E., Grönvold, K., Hilberman, R., Smith, M., Hald, M., December 2002a. High-resolution study of Icelandic tephras in the Kangerlussuaq Trough, southeast Greenland, during the last deglaciation. *Journal of Quaternary Science* 17 (8), 747–757.
- Jennings, A.E., Hald, M., Smith, M., Andrews, J.T., 2006. Freshwater forcing from the Greenland Ice Sheet during the Younger Dryas: evidence from southeastern Greenland shelf cores. *Quaternary Science Reviews* 25 (3–4), 282–298.
- Jennings, A.E., Helgadóttir, G., 1994. Foraminiferal assemblages from the fjords and shelf of Eastern Greenland. *Journal of Foraminiferal Research* 24 (2), 123–144.
- Jennings, A.E., Knudsen, K.L., Hald, M., Hansen, C.V., Andrews, J.T., 2002b. A mid-Holocene shift in Arctic sea-ice variability on the East Greenland Shelf. *The Holocene* 12 (1), 49–58.
- Johnsen, S.J., Dahl-Jensen, D., Gundestrup, N., Steffensen, J.P., Clausen, H.B., Miller, H., Masson-Delmotte, V., Sveinbjörnsdóttir, A.E., White, J., May 2001. Oxygen isotope and palaeotemperature records from six Greenland ice-core stations: Camp Century, Dye-3, GRIP, GISP2, Renland and NorthGRIP. *Journal of Quaternary Science* 16 (4), 299–307.
- Joughin, I., Howat, I., Alley, R.B., Ekstrom, G., Fahnestock, M., Moon, T., Nettles, M., Truffer, M., Tsai, V.C., 2008. Ice-front variation and tidewater behavior on Helheim and Kangerlussuaq Glaciers. *Journal of Geophysical Research* 113 (F01004), F01004.
- Kelley, S.E., Briner, J.P., Young, N.E., 2013. Rapid ice retreat in Disko Bugt supported by ^{10}Be dating of the last recession of the western Greenland Ice Sheet. *Quaternary Science Reviews* 82, 13–22.
- Kelly, M.A., Long, A.J., 2009. The dimensions of the Greenland Ice Sheet since the Last Glacial Maximum. *PAGES News* 17 (2), 60–61.
- Kelly, M.A., Lowell, T.V., 2009. Fluctuations of local glaciers in Greenland during latest Pleistocene and Holocene time. *Quaternary Science Reviews* 28 (21–22), 2088–2106.
- Kelly, M.A., Lowell, T.V., Hall, B.L., Schaefer, J.M., Finkel, R.C., Goehring, B.M., Alley, R.B., Denton, G.H., 2008. A ^{10}Be chronology of lateglacial and Holocene mountain glaciation in the Scoresby Sund region, east Greenland: implications for seasonality during lateglacial time. *Quaternary Science Reviews* 27 (25–26), 2273–2282.
- Kohl, C.P., Nishiizumi, K., 1992. Chemical isolation of quartz for measurement of *in situ*-produced cosmogenic nuclides. *Geochimica et Cosmochimica Acta* 56 (9), 3583–3587.
- Krabill, W., Frederick, E., Manizade, S., Martin, C., Sonntag, J., Swift, R., Thomas, R., Wright, W., Yungel, J., 1999. Rapid thinning of parts of the southern Greenland Ice Sheet. *Science* 283 (5407), 1522–1524.
- Kuijpers, A., Troelstra, S.R., Prins, M.A., Linthout, K., Akhmetzhanov, A., Bouryak, S., Bachmann, M.F., Lassen, S., Rasmussen, S., Jensen, J.B., 2003. Late Quaternary sedimentary processes and ocean circulation changes at the Southeast Greenland margin. *Marine Geology* 195 (1–4), 109–129.
- Lal, D., 1991. Cosmic ray labeling of erosion surfaces: *in situ* nuclide production rates and erosion models. *Earth and Planetary Science Letters* 104 (2–4), 424–439.
- Larsen, H.C., Saunders, A.D., Clift, P.D., Beget, J., Wei, W., Spezzaferri, S., May 1994. Seven million years of glaciation in Greenland. *Science* 264, 952–955.
- Larsen, N.K., Funder, S., Kjær, K.H., Kjeldsen, K.K., Knudsen, M.F., Linge, H., 2013. Rapid early Holocene ice retreat in West Greenland. *Quaternary Science Reviews*.

- Larsen, N.K., Kjær, K.H., Olsen, J., Funder, S., Kjeldsen, K.K., Nørgaard-Pedersen, N., 2011. Restricted impact of Holocene climate variations on the southern Greenland Ice Sheet. *Quaternary Science Reviews* 30 (21), 3171–3180.
- Levy, L.B., Kelly, M.A., Lowell, T.V., Hall, B.L., Hempel, L.A., Honsaker, W.M., Lusas, A.R., Howley, J.A., Axford, Y.L., 2014. Holocene fluctuations of Bregne ice cap, Scoresby Sund, east Greenland: a proxy for climate along the Greenland Ice Sheet margin. *Quaternary Science Reviews* 92 (0), 357–368.
- Lifton, N.A., Bieber, J.W., Clem, J.M., Duldig, M.L., Evanston, P., Humble, J.E., Pyle, R., 2005. Addressing solar modulation and long-term uncertainties in scaling secondary cosmic rays for in situ cosmogenic nuclide applications. *Earth and Planetary Science Letters* 239 (1–2), 140–161.
- Lloyd, J.M., Park, L.A., Kuijpers, A., Moros, M., 2005. Early Holocene palaeoceanography and deglacial chronology of Disko Bugt, West Greenland. *Quaternary Science Reviews* 24, 1741–1755.
- Long, A.J., Roberts, D.H., Simpson, M.J.R., Dawson, S., Milne, G.A., Huybrechts, P., 2008. Late Weichselian relative sea-level changes and ice sheet history in southeast Greenland. *Earth and Planetary Science Letters* 272 (1–2), 8–18.
- Lowell, T.V., Hall, B.L., Kelly, M.A., Bennike, O., Lusas, A.R., Honsaker, W., Smith, C.A., Levy, L.B., Travis, S., Denton, G.H., 2013. Late Holocene expansion of Istorvet ice cap, Liverpool Land, east Greenland. *Quaternary Science Reviews* 63 (0), 128–140.
- Luckman, A., Murray, T., de Lange, R., Hanna, E., February 2006. Rapid and synchronous ice-dynamic changes in East Greenland. *Geophysical Research Letters* 33 (L03503), L03503.
- Lykke-Andersen, H., 1998. Neogene-Quaternary depositional history of the East Greenland shelf in the vicinity of the Leg 152 shelf sites. In: Larsen, H., Saunders, A., Clift, P. (Eds.), *Proceedings, ODP, Scientific Results*, vol. 152, pp. 29–38. College Station, Texas.
- Meier, M.F., Post, A., 1987. Fast tidewater glaciers. *Journal of Geophysical Research: Solid Earth* 92 (B9), 9051–9058.
- Mienert, J., Andrews, J.T., Milliman, J.D., 1992. The East Greenland continental margin (65° N) since the last deglaciation: changes in seafloor properties and ocean circulation. *Marine Geology* 106 (3–4), 217–238.
- Moon, T., Joughin, I., Smith, B., Howat, I., 2012. 21st-Century evolution of Greenland outlet glacier velocities. *Science* 336 (6081), 576–578.
- Murray, T., Scharrer, K., James, T.D., Dye, S.R., Hanna, E., Booth, A.D., Selmes, N., Luckman, A., Hughes, A.L.C., Cook, S., Huybrechts, P., August 2010. Ocean regulation hypothesis for glacier dynamics in southeast Greenland and implications for ice sheet mass changes. *Journal of Geophysical Research: Earth Surface* 115 (F14), F03026.
- Myers, J.S., 1980. Structure of the coastal dyke swarm and associated plutonic intrusions of East Greenland. *Earth and Planetary Science Letters* 46 (3), 407–418.
- Nam, S.I., Stein, R., Grobe, H., Hubberten, H., 1995. Late Quaternary glacial-interglacial changes in sediment composition at the East Greenland continental margin and their paleoceanographic implications. *Marine Geology* 122 (3), 243–262.
- Nielsen, T.F.D., Soper, N.J., Brooks, C.K., Faller, A.M., Higgins, A.C., Matthews, D.W., 1981. The Pre-basaltic Sediments and the Lower Basalts at Kangerdlugssuaq, East Greenland: Their Stratigraphy, Lithology, Palaeomagnetism, and Petrology. Kommissionen for videnskabelige Undersøgelser i Grønland.
- Nishizumi, K., Imamura, M., Caffee, M.W., Sounthorpe, J.R., Finkel, R.C., McAninch, J., 2007. Absolute calibration of ^{10}Be AMS standards. *Nuclear Instruments and Methods in Physics Research Section B: Beam Interactions with Materials and Atoms* 258 (2), 403–413.
- Nutman, A.P., Kalsbeek, F., Friend, C.R.L., 2008. The Nagssugtoqidian orogen in South-East Greenland: evidence for Paleoproterozoic collision and plate assembly. *American Journal of Science* 308 (4), 529–572.
- Ó Cofaigh, C., Dowdeswell, J.A., Jennings, A.E., Hogan, K.A., Kilfeather, A., Hiemstra, J.F., Noormets, R., Evans, J., McCarthy, D.J., Andrews, J.T., Lloyd, J.M., Moros, M., 2013. An extensive and dynamic ice sheet on the West Greenland shelf during the last glacial cycle. *Geology* 41 (2), 219–222.
- Ohmura, A., Reeh, N., 1991. New precipitation and accumulation maps for Greenland. *Journal of Glaciology* 37 (125), 140–148.
- Peirce, B., July 1852. Criterion for the rejection of doubtful observations. *The Astronomical Journal* 2 (21), 161–163.
- Pritchard, H.D., Arthern, R.J., Vaughan, D.G., Edwards, L.A., 2009. Extensive dynamic thinning on the margins of the Greenland and Antarctic ice sheets. *Nature* 461, 971–975.
- Reeh, N., Mayer, C., Miller, H., Thomsen, H.H., Weidick, A., April 1999. Present and past climate control on fjord glaciations in Greenland: implications for IRD-deposition in the sea. *Geophysical Research Letters* 26 (8), 1039–1042.
- Reimer, P., Bard, E., Bayliss, A., Beck, J., Blackwell, P., Bronk Ramsey, C., Buck, C., Cheng, H., Edwards, R., Friedrich, M., Grootes, P., Guilderson, T., Hafidason, H., Hajdas, I., Hatté, C., Heaton, T., Hoffmann, D., Hogg, H., Hughen, K., Kaiser, K., Kromer, B., Manning, S., Niu, M., Reimer, R., Richards, D., Scott, E., Sounthorpe, J., Staff, R., Turney, C., van der Plicht, J., 2013. IntCal13 and Marine13 radiocarbon age calibration curves 0–50,000 years cal BP. *Radiocarbon* 55 (4), 1869–1887.
- Rignot, E., Kanagaratnam, P., 2006. Changes in the velocity structure of the Greenland Ice Sheet. *Science* 311, 986–990.
- Roberts, D.H., Long, A.J., Davies, B.J., Simpson, M.J.R., Schnabel, C., 2010. Ice stream influence on West Greenland Ice Sheet dynamics during the Last Glacial Maximum. *Journal of Quaternary Science* 25 (6), 850–864.
- Roberts, D.H., Long, A.J., Schnabel, C., Freeman, S., Simpson, M.J.R., 2008. The deglacial history of southeast sector of the Greenland Ice Sheet during the Last Glacial Maximum. *Quaternary Science Reviews* 27 (15–16), 1505–1516.
- Roberts, D.H., Rea, B.R., Lane, T.P., Schnabel, C., Rodés, Á., 2013. New constraints on Greenland ice sheet dynamics during the last glacial cycle: evidence from the Uummannaq ice stream system. *Journal of Geophysical Research: Earth Surface* 118 (2), 519–541.
- Ross, S.M., 2003. Peirce's criterion for the elimination of suspect experimental data. *Journal of Engineering Technology* 20, 38–41.
- Sasgen, I., van den Broeke, M., Bamber, J.L., Rignot, E., Sørensen, L.S., Wouters, B., Martinec, Z., Velicogna, I., Simonsen, S.B., 2012. Timing and origin of recent regional ice-mass loss in Greenland. *Earth and Planetary Science Letters* 333–334, 293–303.
- Schjøtt, F., Andresen, C.S., Straneo, F., Murray, T., Scharrer, K., Koralev, A., 2012. Campaign to map the bathymetry of a major Greenland fjord. *EOS, Transactions American Geophysical Union* 93 (14), 141–142.
- Schjøtt, T., 2007a. Kangerdlugssuaq: Gunnbjørns Fjeld/Hvitserk, 1:500,000. In: *Saga Maps Viking Polar Cruise Series*, 1.
- Schjøtt, T., 2007b. Saqqisikuik: Skjoldungen, 1:500,000. In: *Saga Maps Viking Polar Cruise Series*, 1.
- Severinghaus, J.P., Sowers, T., Brook, E.J., Alley, R.B., Bender, M.L., 1998. Timing of abrupt climate change at the end of the Younger Dryas interval from thermally fractionated gases in polar ice. *Nature* 391, 141–146.
- Simpson, M.J.R., Milne, G.A., Huybrechts, P., Long, A.J., 2009. Calibrating a glaciological model of the Greenland ice sheet from the Last Glacial Maximum to present-day using field observations of relative sea level and ice extent. *Quaternary Science Reviews* 28 (17–18), 1631–1657.
- Smith, L.M., Sachs, J.P., Jennings, A.E., Anderson, D.M., de Vernal, A., 2001. Light ^{13}C events during deglaciation of the East Greenland Continental Shelf attributed to methane release from gas hydrates. *Geophysical Research Letters* 28, 2217–2220.
- Sommerhoff, G., 1981. Geomorphologische prozesse in der Labrador-und Irmingersee. Ein Beitrag zur submarinen geomorphologie einer subpolaren meereregion. *Polarforschung* 51 (2), 175–191.
- Sparreborn, C.J., Bennike, O., Björck, S., Lambeck, K., 2006. Holocene relative sea-level changes in the Qaqortoq area, southern Greenland. *Boreas* 35, 171–187.
- Spender, M., 1933. Map-making during the expedition. *Meddelelser om Grønland* 104 (2), 1–21.
- Stein, A.B., 1996. Seismic Stratigraphy and Seafloor Morphology of the Kangerdlugssuaq Region, East Greenland: Evidence for Glaciations to the Continental Shelf Break During the Late Weichselian and Earlier. University of Colorado, Boulder (Master's thesis).
- Stein, R., Nam, S.-I., Grobe, H., Hubberten, H.W., 1996. Late Quaternary glacial history and short-term ice rafted debris fluctuations along the East Greenland continental margin. In: Andrews, J., Austin, W., Bergsten, H., Jennings, A. (Eds.), *Late Quaternary Palaeoceanography of the North Atlantic margins*. Vol. 111 of Geological Society of London, Special Publications, pp. 135–151.
- Stone, J.O., 2000. Air pressure and cosmogenic isotope production. *Journal of Geophysical Research* 105, 23,753–23,760.
- Stoner, J.S., Channell, J.E.T., Hillaire-Marcel, C., March 1995. Magnetic properties of deep-sea sediments off southwest Greenland: evidence for major differences between the last two deglaciations. *Geology* 23 (3), 241–242.
- Straneo, F., Hamilton, G.S., Sutherland, D.A., Stearns, L.A., Davidson, F., Hammill, M.O., Stenson, G.B., Rosing-Asvid, A., 2010. Rapid circulation of warm subtropical waters in a major glacial fjord in East Greenland. *Nature Geoscience* 3 (3), 182–186.
- Straneo, F., Heimbach, P., 2013. North Atlantic warming and the retreat of Greenland's outlet glaciers. *Nature* 504, 36–43.
- Stuiver, M., Reimer, P.J., Reimer, R.W., 2005. CALIB 5.0 (WWW program and documentation).
- Sutherland, D.A., Pickart, R.S., 2008. The East Greenland Coastal Current: structure, variability, and forcing. *Progress in Oceanography* 78 (1), 58–77.
- Sutherland, D.A., Straneo, F., 2012. Estimating ocean heat transports and submarine melt rates in Sermilik Fjord, Greenland, using lowered acoustic Doppler current profiler (LADCP) velocity profiles. *Annals of Glaciology* 53 (60), 50.
- Sutherland, D.A., Straneo, F., Stenson, G.B., Davidson, F.J.M., Hammill, M.O., Rosing-Asvid, A., 2013. Atlantic water variability on the SE Greenland continental shelf and its relationship to SST and bathymetry. *Journal of Geophysical Research: Oceans* 118 (2), 1–9.
- Syvitski, J.P., Jennings, A.E., Andrews, J.T., 1999. High-resolution seismic evidence for multiple glaciation across the Southwest Iceland Shelf. *Arctic, Antarctic, and Alpine Research* 31 (1), 50–57.
- Syvitski, J.P.M., Andrews, J.T., Dowdeswell, J.A., 1996. Sediment deposition in an iceberg-dominated glacimarine environment, East Greenland: basin fill implications. *Global and Planetary Change* 12 (1–4), 251–270.
- Thomas, R., Frederick, E., Krabill, W., Manizade, S., Martin, C., 2009. Recent changes on Greenland outlet glaciers. *Journal of Glaciology* 55 (189), 147–162.
- Thornalley, D.J.R., Elderfield, H., McCave, I.N., February 2009. Holocene oscillations in temperature and salinity of the surface subpolar North Atlantic. *Nature* 457, 711–714.
- Vinther, B.M., Buchardt, S.L., Clausen, H.B., Dahl-Jensen, D., Johnsen, S.J., Fisher, D.A., Koerner, R.M., Raynaud, D., Lipenkov, V., Andersen, K.K., Blunier, T., Rasmussen, S.O., Steffensen, J.P., Svensson, A.M., September 2009. Holocene thinning of the Greenland ice sheet. *Nature* 461, 385–388.
- Vinther, B.M., Clausen, H.B., Fisher, D.A., Koerner, R.M., Johnsen, S.J., Andersen, K.K., Dahl-Jensen, D., Rasmussen, S.O., Steffensen, J.P., Svensson, A.M., 2008. Synchronizing ice cores from the Renland and Agassiz ice caps to the Greenland Ice Core Chronology. *Journal of Geophysical Research: Atmospheres* 113 (D08115), D08115.
- Wager, L.R., Deer, W.A., 1938. A Dyke swarm and crustal flexure in East Greenland. *Geological Magazine* 75 (1), 39–46.
- Wager, L.R., Deer, W.A., Wager, H.G., Manley, G., 1937. The Kangerdlugssuaq Region of East Greenland. *The Geographical Journal* 90 (5), 393–421.

- Weidick, A., Kelly, M., Bennike, O., 2004. Late Quaternary development of the southern sector of the Greenland Ice Sheet, with particular reference to the Qassimiut lobe. *Boreas* 33 (4), 284–289.
- Xu, S., Dougans, A.B., Freeman, S.P.H.T., Schnabel, C., Wilcken, K.M., 2010. Improved ^{10}Be and ^{26}Al -AMS with a 5MV spectrometer. *Nuclear Instruments and Methods in Physics Research Section B: Beam Interactions with Materials and Atoms* 268 (7–8), 736–738.
- Young, N., Schaefer, J.M., Briner, J.P., Goehring, B.M., 2013. A ^{10}Be production-rate calibration for the Arctic. *Journal of Quaternary Science* 28 (5), 515–526.
- Young, N.E., Briner, J.P., Axford, Y., Csatho, B., Babonis, G.S., Rood, D.H., Finkel, R.C., 2011a. Response of a marine-terminating Greenland outlet glacier to abrupt cooling 8200 and 9300 years ago. *Geophysical Research Letters* 38 (24), L24701.
- Young, N.E., Briner, J.P., Rood, D.H., Finkel, R.C., 2012. Glacier extent during the Younger Dryas and 8.2-ka event on Baffin Island, Arctic Canada. *Science* 337 (6100), 1330–1333.
- Young, N.E., Briner, J.P., Stewart, H.A.M., Axford, Y., Csatho, B., Rood, D.H., Finkel, R.C., 2011b. Response of Jakobshavn Isbrae, Greenland, to Holocene climate change. *Geology* 39 (2), 131–134.